Memoirs of the Faculty of Engineering, Nagoya University
Vol.42, No.1 (1990)

A $4\pi\beta$(PPC)-γ(HPGe) COINCIDENCE APPARATUS USING A LIVE-TIMED BI-DIMENSIONAL DATA ACQUISITION SYSTEM AND ITS APPLICATION

Hiroshi MIYAHARA and Chizuo MORI

Department of Nuclear Engineering

(Received May 23, 1990)

Abstract

We constructed a new coincidence apparatus with a live-timed bi-dimensional data acquisition system to the coincidence counting using a $4\pi\beta$ pressurised proportional counter and a high purity germanium gamma-ray detector. This apparatus allowed plural gamma-gate sets in coincidence counting and simultaneous measurement of gamma-ray intensity. Therefore, the disintegration rates of usual sources could be determined quickly and accurately; furthermore, the standardisations of ^{152}Eu and ^{133}Ba which were difficult by coincidence counting could be attained by two-dimensional efficiency extrapolation.

The apparatus was applied to the measurement of gamma-ray emission probability by utilising the effectiveness in simultaneous measurements of disintegration rate and gamma-ray intensity. Gamma-ray emission probability for ^{59}Fe was measured to demonstrate the effectiveness and then the emission probabilities of gamma-rays for ^{86}Rb, ^{103}Ru and ^{42}K were measured. The certainty of the results came up to our expectations.

Contents

1. Introduction 125
2. Experimental equipment 127
3. Measurement of disintegration rate 130
   3.1. Principle of measurement 130
   3.2. Data treatment 132
4. Gamma-ray measurement 133
   4.1. Calculation of peak area 133
   4.2. Measurement of gamma-ray detection efficiency curve 134

5. Results of measurement 137
5.1. Measurement of disintegration rate for nuclide with simple decay scheme 137
5.2. Measurement of disintegration rate of ^{152}Eu 144
5.3. Measurement of disintegration rate of ^{133}Ba 151
5.4. Measurement of the emission probabilities for the 1099 and 1292 keV gamma-rays of ^{59}Fe 157
5.5. Measurement of the emission probability for the 1077 keV gamma-rays of ^{86}Rb 159
5.6. Measurement of the emission probabilities for the 497, 557 and 610 keV gamma-rays of ^{103}Ru 161
5.7. Measurement of the emission probability for the 1525 keV gamma-rays of ^{42}K 165
6. Conclusion 168
Acknowledgements 169
References 169

1. Introduction

The probability of gamma-rays with particular energy emitted per one decay of a radioisotope, or gamma-ray emission probability, is an important factor in the research field of nuclear-reaction products or radioisotope application. The term, gamma-ray intensity, used till the 1970's ordinarily meant the relative intensity of gamma-rays emitted by the decay. At that time, the term, absolute gamma-ray intensity, was specifically used as the same meaning as the gamma-ray emission probability used at present. The users of these data usually required not only relative gamma-ray intensity but also the emission probability. The relative gamma-ray intensity could be measured without much difficulty, but the emission probability could not be determined with ease. In this context, the relative gamma-ray intensity was measured mainly in the field of nuclear physics. Extremely speaking, the measurement of disintegration rate has belonged to the field different from the gamma-ray measurement, then it has been difficult to carry out simultaneously both measurements.

The relative gamma-ray intensity can be measured with considerably high accuracy after the development of gamma-ray semiconductor detector with high energy-resolution, and it has been measured for the nuclides with various half-lives. Among the results measured in earlier time, some data are not confident and lose propriety in designation of certainty. In beta-decay nuclides, the probability of beta transition to the ground state is significantly important to calculate the gamma-ray emission probability from the relative gamma-ray intensity. This situation is similar to electron capture-decay nuclides and alpha-decay ones. In the case of no direct decay to the ground state, gamma-ray emission probability can be determined by calculating the income and outgo of each energy level from the relative gamma-ray intensities and internal conversion coefficients. However in the case that the probability of direct decay to the ground level is not zero, the gamma-ray emission probability cannot be determined from only the relative gamma-ray intensity without beta transition data.

Calibration of gamma-ray detection efficiency is required also for the measurement of relative gamma-ray intensity; therefore, the standard sources with the accurately determined disintegration rates are inevitably required. The certainty of easily obtainable standard sources ranges from 2% to 5%, then on the calibration of gamma-ray detection efficiency with high certainty we must use the standard sources of which the disintegration rates are determined by ourselves or by metrologist, as for example Schotzig et al.[1], Gehrke et al.[2] and Yoshizawa et al.[3] did. Measurement of disintegration rate with high certainty is usually carried out by efficiency extrapolation method for the coincidence efficiency function obtained

from $4\pi\beta$-γ coincidence counting for beta-decay and electron capture-decay nuclides. The $4\pi\beta$ counter detects beta-rays or Auger electrons and X-rays. A conventional automatic measurement requires about one day for one source, and the disintegration rates of plural sources for calibration of gamma-ray detection efficiency took a long time and could not be measured without much efforts. In such a situation, it is very difficult work to measure the disintegration rates of these sources every time.

We have reported that the application of bi-dimensional data acquisition system to the $4\pi\beta$-γ coincidence counting brings the quick measurement of coincidence efficiency function and then the determination of the disintegration rate[4]. Basically, the whole points of the coincidence function in this method can be obtained from the measured data correspond to one point of that in conventional method, by using computer discrimination method[5]. Then the equivalent result to conventional one is attained in shorter time less than one tenth of conventional counting time. This method allows plural gate sets for optional gamma-rays after finishing the measurement; therefore, the disintegration rate of the source can be determined simply, quickly and accurately. Furthermore, we can simultaneously obtain gamma-ray spectrum by this system. A NaI(Tl) scintillator was used as the gamma-ray detector in the experiment reported before[4], because the subject in that experiment was only the measurement of disintegration rate. A gamma-ray semiconductor detector must be used to attain high-resolution energy spectrum of gamma-rays. The combination of a $4\pi\beta$(ppc)-γ(HPGe) coincidence apparatus and a live-timed bi-dimensional data acquisition system makes it possible to measure simultaneously both the disintegration rates and gamma-ray spectra of standard sources for calibration of detection efficiency of the HPGe detector. Simultaneous measurements of disintegration rate and gamma-ray spectrum of a sample nuclide for which it was difficult to determine precisely the gamma-ray emission probability so far bring the possibility of the precise determination.

A $4\pi\beta$(ppc)-γ(HPGe) coincidence apparatus was manufactured and incorporated with the live-timed bi-dimensional data acquisition system for the determination of precise gamma-ray emission probability. This system required not only the substitution of an HPGe detector for the NaI(Tl) scintillation detector in $4\pi\beta$(ppc)-γ(NaI(Tl)) coincidence apparatus using a live-timed bi-dimensional data acquisition system, but also the construction of a new $4\pi\beta$ pressurised proportional counter ($4\pi\beta$(ppc)) under consideration of gamma-ray measurement and a stand to fix relative geometrical position of both detectors. Coincidence counting requires an amplifier with short time constant. On the contrary high energy-resolution gamma-ray measurement using the HPGe detector requires one with relatively long time constant; therefore, it necessitates more complex electronic system than that used in the $4\pi\beta$(ppc)-γ(NaI(Tl)) coincidence apparatus using the live-timed bi-dimensional data acquisition system.

Manufacturing the whole equipment, we first measured the disintegration rates of some nuclides with simple decay schemes and established the new method to be reliable for the measurement of the disintegration rate by comparing the results with those obtained from conventional counting. The disintegration rates for ^{152}Eu and ^{133}Ba which are useful multi-gamma sources for calibration of detector could be measured by utilising the characteristics of this system that the computer discrimination method was able to be applied for the plural gamma-ray gates. These nuclides decay by electron capture process and emit large amounts of internal conversion electrons, and ^{152}Eu is the nuclide that is difficult to measure its activity by the $4\pi\beta$-γ coincidence counting and ^{133}Ba is the one that the extrapolated values obtained from the $4\pi\beta$-γ coincidence counting changes for different gamma-ray gates. Therefore, the precise measurement of the disintegration rates of these sources is especially desired for the detection efficiency calibration of HPGe detectors.

After the measurements of detection efficiencies using the sources with simple decay

schemes and the above described multi-gamma sources, gamma-ray emission probabilities were measured for some nuclides. The emission probabilities for principal gamma-rays of ^{59}Fe were measured to demonstrate the effectiveness of this system because this nuclide had small direct beta decay to the ground state. The probability of beta decay to the ground state calculated from the results showed the appropriateness and certainty of this method. The gamma-ray emission probability of ^{86}Rb which has 90% direct beta decays to the ground state was measured as an object to make the most of the characteristics of this system and to examine the limit of it. ^{103}Ru decays to the ground level or the 40 keV metastable level with half life of 56 min and the most of the transition from the 40 keV level are internally converted. There were then many problems in the measurements of disintegration rate and gamma-ray emission probability. Although ^{42}K decays with short half life of about 12 h, the gamma-ray emission probability could be determined precisely by this system owing to the simultaneous measurement of disintegration rate and gamma-ray spectrum.

2. Experimental equipment

An equipment is composed of a $4\pi\beta$ pressurised proportional counter ($4\pi\beta$(ppc)), a high purity germanium (HPGe) detector and coincidence apparatus using a live-timed bi-dimensional data acquisition system. The HPGe detector is the horizontal type of 14% efficiency (44.6 mm dia and 50.0 mm length) or 23% efficiency (56.4 mm dia and 48.0 mm length). Thus the gamma-ray detector is exchangeable without bringing any inconvenience, because the detector is calibrated in every measurement of gamma-ray emission probability.

The $4\pi\beta$(ppc) was manufactured under the following condition. High count rate of gamma-rays is desired from the statistical standpoint for precise measurement using the HPGe detector, but cascade summing effect increases when high efficiency is obtained by decreasing the distance between source and detector. Usually, the source is positioned apart more than 10 cm from the detector and there is minimum amount of substance to interact with gamma-rays between them. High count rate of gamma-rays is desirable for precise determination of the disintegration rate with $4\pi\beta$-γ coincidence counting. The distance had to be determined by compromising between them and the absorption due to the wall of $4\pi\beta$(ppc) had to be decreased reasonably. The two $2\pi\beta$ counters used in the $4\pi\beta$(ppc)-γ(NaI(Tl)) coincidence counting system[4] were made of brass with sensitive volume of $40 \times 20 \times 40$ mm^3 and operated at 1.3 MPa, whereas the counters in the new system were made of aluminum to decrease the absorption of gamma-rays.

The source-detector distance was compromised with 7 cm for the detector with 14% efficiency and with 9 cm for the one with 23% efficiency, and the distance restrained the cascade summing correction to be within 2% and the uncertainty to be within 0.1%. It was satisfied that the uncertainty of final result was within 1%. The relatively large distance allowed to manufacture a large $4\pi\beta$(ppc) composed of aluminum and to operate at relatively low gas pressure (0.5 to 0.7 MPa), because high energy beta-rays deposited enough energy in the gas. Furthermore, to decrease absorption of gamma-rays the counter wall in the path from the source to the detector was made thinner (5 mm) than the other part (10 mm).

Fig. 2-1 shows the sketch of the $4\pi\beta$(ppc). Both $2\pi\beta$ counters had sensitive volumes of $80 \times 40 \times 80$ mm^3 and a source was put between them. Since the reproducibility of source position affects the accuracy of gamma-ray detection efficiency, no space was planed between source mounts and metal ring to support the source. The anodes were stainless steel wire of 22 μm dia. The counter was operated at 0.6 to 0.7 MPa of a 90% argon-10% methane

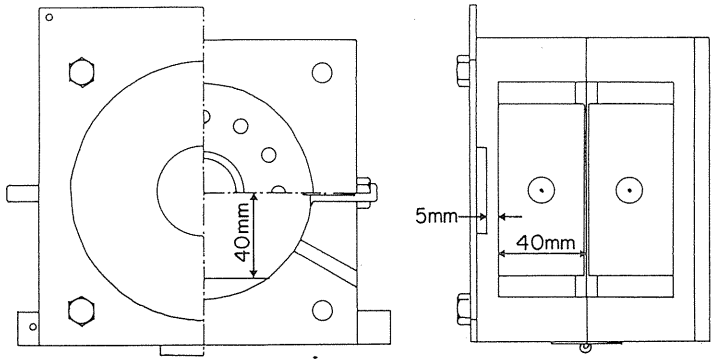

Fig. 2-1. A schematic diagram of a $4\pi\beta$ pressurised proportional counter.

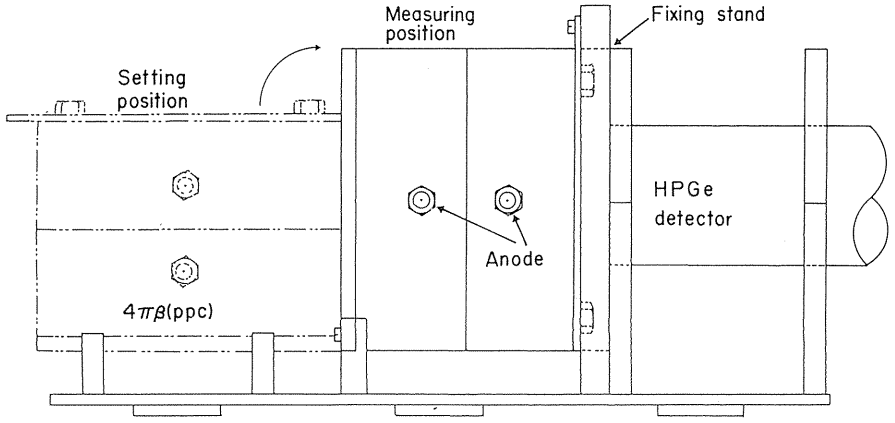

Fig. 2-2. Arrangement of a $4\pi\beta$(ppc) and an HPGe detector and a stand to fix. When an HPGe detector with relative detection efficiency of 23% is used, it is fixed further about 2 cm compared with 14% detector.

mixture (P-10 gas). The high voltage of 3.5 and 3.8 kV must be applied to obtain gas amplification of a few hundreds at 0.6 and 0.7 MPa, respectively[6].

The $4\pi\beta$(ppc) must be fixed against the HPGe detector with geometrically good reproducibility. As the HPGe detectors were the horizontal type, the source was measured in vertical position. However, the source must be placed horizontally when it is mounted in the counter. Fig. 2-2 shows the fixing stand together with both detectors. After the source was set horizontally in the counter, the counter was raised and fixed to the stand composed of brass for the measurement. The HPGe detector was also fixed to the stand by using acrylic resin board. The whole detection system was shielded by lead blocks with 5 cm thickness.

Sources had the same form as that used for ordinary $4\pi\beta$ counting; a VYNS (copolymer of vinyl acetate and vinyl chloride) film stretched on a brass mount with 39 mm outer diameter, 15 mm inner diameter and 0.3 mm thickness was metallised by evaporation of gold-palladium and a source was prepared on it by aluminum treatment method[7].

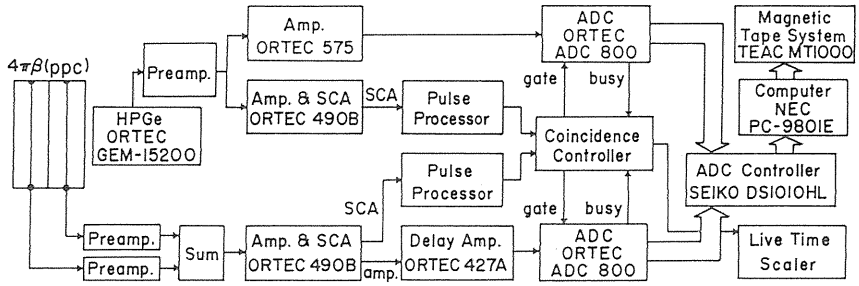

Fig. 2-3. A block diagram of the electronics for the live-timed bi-dimensional data acquisition system composed of the $4\pi\beta$(ppc) and the HPGe detector.

Fig. 2-3 shows the block diagram of the electronics. Basic function of the electronics was to record pulse heights and relative time relation of beta and gamma signals from both detectors on a magnetic tape. The live time was simultaneously measured for the important correction in computer analysis. When a NaI(Tl) scintillator was used as the gamma-ray detector, it was enough to use amplifiers with single-channel pulse-height analyser in both channels. An HPGe detector, however, required usually the amplifier with long time constant to attain high-resolution gamma-ray measurement, then the peak in pulse shape was appeared at late time and variation of the time was relatively large. The amplifier was not fundamentally fit for coincidence counting which required precise time relation; therefore, the electronics shown in the figure was necessary.

Signals from each detector through preamplifier are amplified and discriminated by Ortec 490B amplifier to judge the coincidence relation, and the digital outputs go to a home-made coincidence controller. The coincidence controller determines single or coincident event within the resolving time for all signals. If the signal is judged to be a single event, it outputs a pulse delayed by the resolving time to the anticoincidence gate of another channel's ADC (Ortec 800) and stops the function of the ADC. If the signals are judged to be coincident events, it outputs no pulse and each ADC analyses the pulse height of each analog input.

An ADC controller (SEIKO DS1010HL) has functions to judge coincidence or anti-coincidence and to output informations of channel, pulse height and time relation to a micro-computer (NEC PC-9801E). After the data of 2^{12} events are stored on a dynamic random-access memory (DRAM) in the computer, the data are written on a magnetic tape and following data are stored in another DRAM. Precise resolving time, however, cannot be set in the ADC controller and the judgement of coincidence for the signals from the amplifier with long time constant brings uncertainty; therefore, the resolving time is set long enough and the coincidence controller works predominantly for the judgement of coincidence. When signals are detected simultaneously in beta and gamma channels, the analog and the digital signals in both channels must reach the coincidence controller and both ADCs at the same time. The analog signal from the second amplifier (Ortec 575) which is used for high-resolution gamma-ray spectrometry in the gamma channel reaches its peak at the time delayed from other signals by about 3 μs. The analog signal in the beta channel is delayed 2.75 μs by a delay amplifier (Ortec 427A) and the digital signals in both channels are delayed by originally-made pulse processors. Good adjustment for the timing of both digital signals is important to minimise Gandy effect[8]. Timing adjustment between the peak of analog signal and digital signal is difficult. However, precise coincidence is not necessary for bi-dimensional

data acquisition system, but it is necessary that the peak of analog signal appears always within a constant time from the digital signal. A busy signal from the ADC during the pulse height analysis closes the input gate of the coincidence controller not to accept the digital signals of both channels.

The coincidence controller has the function to measure live time. It contains a pulser to generate 10 kHz pulses and outputs the pulses to a live-time scaler only during the time in which both ADCs are not operating (no busy signal from both ADCs). The live time measured by the scaler, therefore, means the time that both ADCs are live, then it is slightly different from live time of each channel. The live time of each channel is calculated from the live time measured and it will be described in detail at the section of data treatment.

3. Measurement of disintegration rate

The method to determine the disintegration rate of a source from measured data is the same as that in the conventional counting, but the coincidence efficiency function for each source can be determined by the computer discrimination method. The problem different from the conventional coincidence counting is the treatments of long dead time. These treatments are described in this chapter.

3. 1. Principle of measurement

When conventional $4\pi\beta$-γ coincidence counting is applied to a nuclide which emits gamma-rays and internal conversion electrons (coefficient α) following beta decay, the following equations are obtained[9].

$$n_\beta = n_0 \left[\varepsilon_\beta + (1 - \varepsilon_\beta) \frac{\alpha\, \varepsilon_{ce} + \varepsilon_{\beta\gamma}}{1 + \alpha} \right] \tag{3-1}$$

$$n_\gamma = n_0 \left[\frac{\varepsilon_\gamma}{1 + \alpha} \right] \tag{3-2}$$

$$n_c = n_0 \left[\frac{\varepsilon_\beta\, \varepsilon_\gamma}{1 + \alpha} + (1 - \varepsilon_\beta)\, \varepsilon_{cc} \right] \tag{3-3}$$

where n_0 is the disintegration rate, n_β, n_γ, n_c are the beta, the gamma, the coincidence count rates, ε_β, ε_γ are the beta, the gamma detection efficiencies, ε_{ce}, $\varepsilon_{\beta\gamma}$ are the detection efficiencies of beta counter for the internal conversion electrons and gamma-rays, and ε_{cc} is the probability of γ-γ coincidence. When the gamma gate is set on the photopeak, the following relation is derived by neglecting ε_{cc}.

$$\frac{n_\beta \cdot n_\gamma}{n_c} = n_0 \left[1 + \frac{1 - \varepsilon_\beta}{\varepsilon_\beta} \left(\frac{\alpha\, \varepsilon_{ce} + \varepsilon_{\beta\gamma}}{1 + \alpha} \right) \right]. \tag{3-4}$$

If ε_{ce} and $\varepsilon_{\beta\gamma}$ are constant, Eq. (3-4) changes linearly with $(1-\varepsilon_\beta)/\varepsilon_\beta$ and $\varepsilon_\beta \to 1$ yields $n_\beta n_\gamma / n_c \to n_0$. Therefore, a series of $4\pi\beta$-γ coincidence countings under the different beta efficiencies gives the practical relation shown in Eq. (3-4) (coincidence efficiency function) and the disintegration rate is determined by the extrapolation $(1-\varepsilon_\beta)/\varepsilon_\beta \to 0$.

The $4\pi\beta$-γ coincidence counting can be applied to the measurement of nuclides with complex decay scheme, then the individual channel count rates are expressed as the summing of each branch by the following[10],

$$n_\beta = n_0 \sum a_k \left[\varepsilon_{\beta k} + (1 - \varepsilon_{\beta k}) \left(\frac{\alpha\, \varepsilon_{ce} + \varepsilon_{\beta\gamma}}{1 + \alpha} \right)_k \right] \tag{3-5}$$

$$n_\gamma = n_0 \sum a_k\, \varepsilon_{\gamma k} \left(\frac{1}{1 + \alpha} \right)_k \tag{3-6}$$

$$n_c = n_0 \sum a_k \left[\varepsilon_{\beta k}\, \varepsilon_{\gamma k} \left(\frac{1}{1 + \alpha} \right)_k + (1 - \varepsilon_{\beta k})\, \varepsilon_{ck} \right] \tag{3-7}$$

$$\frac{n_\beta \cdot n_\gamma}{n_c} = n_0 \left[1 + \frac{1 - \varepsilon_\beta}{\varepsilon_\beta} \{1 - \sum a_k\, C_k \left[1 - \left(\frac{\alpha\, \varepsilon_{ce} + \varepsilon_{\beta\gamma}}{1 + \alpha} \right)_k \right] \} \right] \tag{3-8}$$

where

$$C_k = \frac{1 - \varepsilon_{\beta k}}{1 - \varepsilon_\beta}, \quad \varepsilon_\beta = \frac{n_c}{n_\gamma}$$

the suffix k and a_k show the k-th beta branch and the fractional intensity, and ε_{ck} is neglected in Eq. (3-8) on the above consideration. The ε_β means the detection efficiency for the beta branch followed by gamma-rays of which the photopeak is selected to set the gate. If ε_{ce}, $\varepsilon_{\beta\gamma}$ and C_k are constant, the coincidence efficiency function is obtained from the measurements with different beta efficiencies around 1 of ε_β and the linear extrapolation yields the disintegration rate n_0.

A pulse height discrimination method is one of those to measure the coincidence efficiency function and gives the results with different beta efficiencies by changing the discrimination level of beta channel. In the pulse height discrimination method, the proportionality between beta-ray energy and the pulse height is required to keep C_k constant[11], a $4\pi\beta$(ppc) is therefore usually used to keep the proportionality between them. To obtain the coincidence efficiency function sufficient to extrapolate, several tens measurements must be repeated under the condition of different discrimination levels. On a computer discrimination method[5], the beta spectrum and the coincident one are stored by using a multi-channel pulse height analyser instead of the pulse height discriminator. After the measurement the pulse height discrimination process by changing the discrimination level with computer program gives many results of coincidence counting with different beta efficiencies and the disintegration rate is determined by the extrapolation.

A $4\pi\beta$(ppc)-γ(NaI(Tl)) coincidence apparatus using a live-timed bi-dimensional data acquisition system is an extension of this principle and have already reported[4]. The ordinary computer discrimination method measures the beta spectrum and the one coincident with gated gamma signals. The utilisation of bi-dimensional data acquisition system is, on the other hand, able to measure three-dimensional spectrum with both axes of gamma-ray spectrum and beta-ray spectrum. This method allows many gamma gates against one or two gates in the ordinary method. The equipment described in section 2 is used for the measurement of three dimensional spectrum where an HPGe detector is fabricated as a gamma detector and the simultaneous measurements of coincidence counting and gamma-ray intensity is possible.

3. 2. Data treatment

The following is the procedure for calculating the disintegration rate from the data on a magnetic tape.

1. Determining the lower and upper channels for some gamma gates.
2. Reading out the data from the magnetic tape and accumulating beta and gamma spectra and the spectra of beta signals which coincide with all gamma signals and with gamma signals in the gates determined in procedure 1.
3. Calculating live times to obtain the count rate in each spectrum.
4. Correcting the chance coincidence.
5. Determining the background spectra and subtracting them from the above spectra.
6. Calculating gamma-ray count rate contained in the gate channels from the gamma-ray spectrum (n_γ).
7. Summing the count rates above i-th channel in the beta spectrum and the one in beta signals coincided with gamma signals within the gate ($n_{\beta i}$, n_{ci}).
8. Calculating beta-ray detection efficiency ($\varepsilon_{\beta i}=n_{ci}/n_\gamma$) and apparent disintegration rate ($n_{\beta i}n_\gamma/n_{ci}$).
9. Repeating the procedures 7 and 8 under the different conditions with different starting channels (i) for the determination of coincidence efficiency function and disintegration rate (n_0) by efficiency extrapolation.

Each procedure is described in detail as follows; the gamma gate channels to select arbitrary photopeaks in procedure 1 are determined from the gamma spectrum obtained from a part of the data stored on the magnetic tape. About 2×10^7 events stored on a 732 m magnetic tape are analysed in procedure 2 and plural beta spectra coincided with gamma signals in the gates are obtained in the case of plural gate setting.

In the coincidence controller, a digital pulse of one channel arrived first inhibits to pass the following pulse of the channel and the pulse of the other channel after the resolving time (T_R), then the counts of live-time scaler (T_L) show the time to be live in both ADCs. Therefore, the total live time of each channel ($T_{L\beta}$, $T_{L\gamma}$, T_{LC}) is calculated as following.

$$T_{L\beta} = T_L + T_R\,(N'_{\gamma a} - N'_{ca}) \tag{3-9}$$

$$T_{L\gamma} = T_L + T_R\,(N'_{\beta a} - N'_{ca}) \tag{3-10}$$

$$T_{LC} = T_L \tag{3-11}$$

where $N_{\beta a}$, $N_{\gamma a}$ and N_{ca} are the total counts of beta, gamma and coincidence which are obtained by summing the beta, gamma spectra and beta spectrum coincided with all gamma signals, and a symbol ($'$) means the counts including background.

Principally, a coincidence efficiency function is calculated from two spectra of beta and coincident beta signals and the total counts of gamma signals selected. However, the correction for accidental coincidence is required for all beta signals and all gamma signals. The well-known correction formula[9] for accidental coincidence is

$$n_c = \frac{n_c^* - 2\,T_R n'_\beta\, n'_\gamma}{1 - T_R(n'_\beta + n'_\gamma)} \tag{3-12}$$

where n_c^* is coincidence count rate corrected for background. Procedure 4 for the case of bi-dimensional coincidence must be executed for each site of i-th beta channel and j-th gamma

channel. Therefore, the correction formula is

$$n_{cij} = n^*_{cij} - \left\{ n_{ca} - \frac{n^*_{ca} - 2\,T_R n'_{\beta a} n'_{\gamma a}}{1 - T_R(n'_{\beta a} + n'_{\gamma a})} \right\} \frac{n'_{\gamma j} n'_{\beta i}}{n'_{\gamma a} n'_{\beta a}} \tag{3-13}$$

The procedures 5 to 9 are simple operations and it is easy to put previously the repetition of procedures 7 and 8 in the calculation program. The results are the similar ones obtained from conventional coincidence counting, then the disintegration rate is determined from the efficiency function by extrapolation.

4. Gamma-ray measurement

The gamma-ray spectrum can be obtained from the data treatment described in section 3.2 together with the coincidence efficiency function. The spectrum gives gamma-ray intensities which determine the detection efficiencies of the HPGe detector and gamma-ray emission probabilities. Though the data treatment and the calculation method are not different from ordinary gamma-ray measurement, the procedure used in this experiment is described in the following.

4. 1. Calculation of peak area

An HPGe detector shows high energy-resolution in gamma-ray measurement, then a sharp peak is observed at the position of total energy loss. Therefore, it is less serious problem for the spectrum from the HPGe detector than for that from the NaI(Tl) detector to estimate the continuous spectrum under the peak for calculation of peak area. The continuous component, however, affects largely the uncertainty of peak area, then serious consideration on the component is necessary to determine precisely the gamma-ray intensity.

It is widely used that the measured data in the region of a peak are fitted with an analytical function assumed for the calculation of the peak area. The function is composed of the sum of a Gaussian function representing the peak and 1st or 2nd linear function representing the continuum. Practically, to represent the peak shape containing low-energy tail and complex continuum, non-linear fitting using more complex function is required. Dojo[12] obtained good result by using an exponential tail for lower-energy side and an error function for the step of continuum. The complex peak function, however, requires tedious calculation, then an integral method is sometimes used instead of non-linear fitting. The spectral analysis described by Helmer[13] was introduced in this study.

The first approximation value S_0 of peak area is calculated from the assumed continuum of line $b(x)$ connecting both edge points A and B of a peak, shown in Fig. 4-1.

$$S_0 = \int_A^B \{y(x) - b(x)\}\, dx \tag{4-1}$$

The value of continuum $B(x)$ at channel x is approximated by using the above result.

$$B(x) = \frac{\int_A^x \{y(z) - b(z)\}\, dz}{S_0} \{y(B) - y(A)\} + y(A) \tag{4-2}$$

In the second approximation the peak area S is obtained as follows.

$$S = \int_A^B \{y(x) - B(x)\}\, dx \tag{4-3}$$

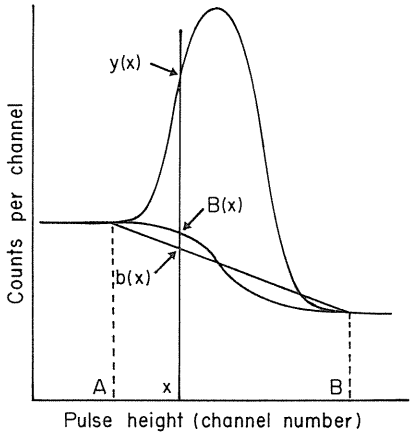

Fig. 4-1. A typical peak fitting by summation method. The curves of $b(x)$ and $B(x)$ show a first and a second approximated continuous components, respectively.

If the exponential tail contributes little and the peak is composed of the sum of a Gaussian, an error function and a constant, this method is nearly equal to Dojo's non-linear fitting. Furthermore, the calculation by computer is simple and gives converged value through only a few repetitions. Five time repetition process is adopted in the practical calculation.

A systematic uncertainty of peak area due to this method depends largely on the determination of the peak-edge channels. When peak areas were calculated by increasing intentionally the peak-edge channels for a practical spectrum, the variations among them were about 0.1% of the area. However, the contribution of low-energy tail increased gradually in the case of no continuum, then the systematic uncertainty of this method may be estimated to be about 0.3%.

4. 2. Measurement of gamma-ray detection efficiency curve

The gamma-ray intensity emitted from a source can be determined from the peak area decided by the method described in the previous section, when the peak efficiency of the detector is already known. Therefore, the efficiency function giving the relation between gamma-ray energy and detection efficiency must be measured. When $4\pi\beta$-γ coincidence counting using the live-timed bi-dimensional data acquisition system is carried out for the nuclides with well-known gamma-ray emission probabilities, the detection efficiency for a gamma-ray energy is easily obtained from the determined disintegration rate and the peak area. If some detection efficiencies obtained at suitable energy intervals by using a few kinds of nuclides are functionalised, the efficiency function gives the detection efficiency and the expected uncertainty at desired gamma-ray energy.

Sources of ^{46}Sc, ^{57}Co, ^{60}Co, ^{88}Y, ^{133}Ba, ^{134}Cs and ^{152}Eu were used for the calibration of the detection efficiency of the HPGe detector. Sources of ^{54}Mn, ^{57}Co, ^{60}Co and ^{137}Cs were used for the measurement of the total detection efficiency that was required for cascade summing correction described in the latter. The disintegration rates of these nuclides were

measured partly by the method described in section 3 and partly by that described in section 5. Cascade summing correction that is necessary for the determination of the detection efficiency from the peak area is discussed here. When the gamma-rays emitted in cascade are detected simultaneously, the energy information of each gamma-ray disappears and the spectrum is obtained as if the gamma-ray with the sum energy is detected. Therefore, the distorted peak area must be corrected.

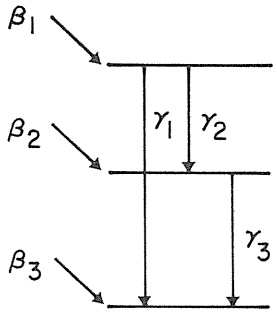

Fig. 4-2. A schematic decay scheme to consider the cascade summing effect.

The principle of this correction may be illustrated by considering the simple decay scheme of Fig. 4-2. When γ_2 and γ_3 simultaneously deposit their full energy in the detector, they contribute to the peak of γ_1 and must be subtracted from the recorded peak area $n'(\gamma_1)$. The corrections for the peaks of γ_2 and γ_3 are of another type. The recorded peak areas $n'(\gamma_2)$ and $n'(\gamma_3)$ are smaller than they should be. Since each γ_2 is followed by γ_3 in coincidence, detection of both gamma-rays leads to a single pulse. If the energy of γ_2 is totally absorbed and that of γ_3 is partially absorbed, the event is lost from the peak of γ_2. The situation for the peak of γ_3 is somewhat different, because γ_3 is not always preceded by γ_2 like as depicted in Fig. 4-2. If it is assumed that there is no angular correlation between them, here we get

$$n'(\gamma_1) = n_0 P_1 \varepsilon_1 + n_0 P_2 \varepsilon_2 \varepsilon_3 = n(\gamma_1) + n(\gamma_2)\, \varepsilon_3 \tag{4-4}$$

$$n'(\gamma_2) = n_0 P_2 \varepsilon_2 - n_0 P_2 \varepsilon_2 \varepsilon_3^{\,t} = n(\gamma_2) - n(\gamma_2)\, \varepsilon_3^{\,t} \tag{4-5}$$

$$n'(\gamma_3) = n_0 P_3 \varepsilon_3 - n_0 P_3 \varepsilon_3 \frac{P_2}{P_3} \varepsilon_2^{\,t} = n(\gamma_3) - n(\gamma_3) \frac{P_2}{P_3} \varepsilon_2^{\,t} \tag{4-6}$$

where $n(\gamma_i)$ is the expected true peak count rate of γ_i, P_i is the emission probability of γ_i, ε_i is the full-energy peak efficiency and superscript t shows the total efficiency. The correction factor for each gamma-ray is obtained from Eqs. (4-4) to (4-6).

$$C_1 = \frac{n(\gamma_1)}{n'(\gamma_1)} = \frac{1}{1 + P_2 \varepsilon_2 \varepsilon_3 / P_1 \varepsilon_1} \tag{4-7}$$

$$C_2 = \frac{n(\gamma_2)}{n'(\gamma_2)} = \frac{1}{1 - \varepsilon_3^{\,t}} \tag{4-8}$$

$$C_3 = \frac{n(\gamma_3)}{n'(\gamma_3)} = \frac{1}{1 - P_2 \varepsilon_2^{\,t} / P_3} \tag{4-9}$$

Generally, the correction factor for the nuclide emitting multi-gamma rays is following[14].

$$C_i = \frac{n(\gamma_i)}{n'(\gamma_i)} = \frac{1}{1 - \sum K_j \varepsilon_j' + \sum P_{jk} \varepsilon_j \varepsilon_k / P_i \varepsilon_i} \tag{4-10}$$

where K_j is the relative intensity of j-th gamma-rays which are coincident with i-th gamma-rays and P_{jk} is the emission probability of j- and k-th gamma-rays that both gamma-rays are the cascade relation and sum of both energies is equivalent to the energy of i-th gamma-rays.

Thus, the important factor for cascade-summing correction is the total detection efficiency. As the correction for cascade summing is smaller than 2% in this system, the total detection efficiency must be determined within the uncertainty of 5% to suppress the uncertainty of the correction of cascade summing for peak efficiency within 0.1%. Therefore, the following method was used for the determination of total detection efficiency. The peak efficiencies and the total efficiencies were measured for the mean energies of ^{57}Co and ^{60}Co. The peak-to-total ratios were measured for ^{54}Mn and ^{137}Cs. The total efficiencies for them were calculated from those ratios and the tentative peak efficiencies obtained by using the

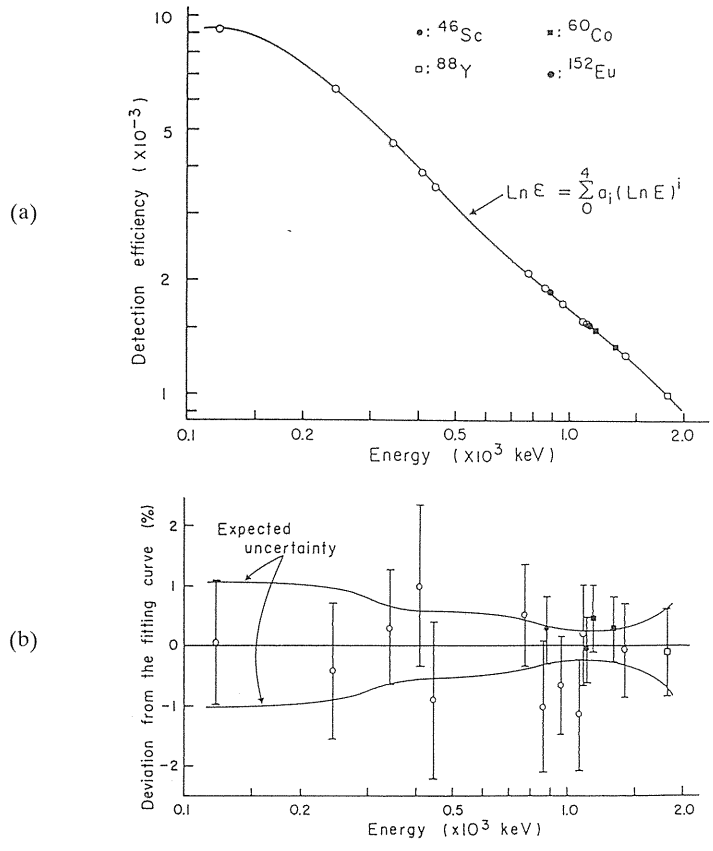

Fig. 4-3. An example of detection efficiency (a) and deviation (b) from the fitting function. The solid lines in (b) show the expected standard deviation.

peak efficiency function without correction of cascade summing. The total efficiency function was determined by fitting these tentatively calculated values to the relative total efficiency function calculated using only the absorption coefficients. Then, by using the total efficiency function the peak efficiency function corrected for cascade summing was determined. Repetition of these procedures gave the converged reliable total detection efficiency function and the correction factor for cascade summing could be correctly calculated. Then the true detection efficiencies were determined by multiplying the apparent detection efficiencies and the correction factors for cascade summing. The true detection efficiencies with standard deviations must be fitted on a particular function. The standard deviation used for calculation was sum of the statistical uncertainties and the systematic uncertainties mentioned as following. The uncertainty due to the geometrical arrangement was 0.3% under the estimation of the reproducibility of source position to be 0.1 mm, that due to the evaluation of peak area 0.3%, that due to the neglect of the chance coincidence 0.1%, that dependent on the uncertainty of time measurement of live-time 0.1%, and that due to the correction for cascade summing was estimated to be 5% of the correction. The fourth-order polynomial function of both logarithmic scales was used for fitting the detection efficiencies of the standard sources by the method of least squares using a covariance matrix described by Brandt[15]. An example of the result is shown in Fig. 4-3 with the deviation of the measured data from the fitting function. The solid lines show the estimated standard deviation accompanied with the detection efficiency derived from the fitting function.

5. Results of measurement

The previous sections dealt with general articles of disintegration rate measurement and gamma-ray measurement. In this section, the disintegration rate measurement of individual isotopes and the results of gamma-ray emission probabilities for particular nuclides will be described.

5. 1. Measurement of disintegration rate for nuclide with simple decay scheme

Measurement of disintegration rate for ^{60}Co is important for all utilisation. ^{60}Co scarcely emits internal conversion electrons, then the $4\pi\beta$(ppc) detects only the gamma-rays of ^{60}Co with efficiency of about 10^{-3} except for beta-rays. Therefore, the coincidence efficiency function corresponding to Eq. (3-4) should be nearly straight line with slope of 10^{-3}, when the gamma gate is set on the full-energy peak of 1333 keV gamma-rays. Actually measured beta spectrum and that coincident with 1333 keV gamma-rays are shown in Fig. 5-1 and the coincidence efficiency function is shown in Fig. 5-2. The continuous spectrum below 40 keV shown in Fig. 5-1 gives nearly constant distribution and beta-rays deposited much energy in the gas form the peak positioned at right edge. The coincidence efficiency function showed small slope as expected, and it was natural from considering the standard deviation that negative slope was occasionally observed. As the best detection efficiency was about 0.95 for ^{60}Co, the correction of extrapolation was calculated to be about 0.03%. Therefore, the calculated result without extrapolation showed only the systematic uncertainty less than 0.05%. Fig. 5-3 shows the comparison of the results measured by this system and by ordinary system using a NaI(Tl) scintillator. The mean value of the results by this method agrees with the result obtained from the ordinary counting within the standard deviation.

The coincidence efficiency function of ^{60}Co shows no significant slope because of one beta branch and because of no conversion electron. On the contrary, ^{134}Cs which has main

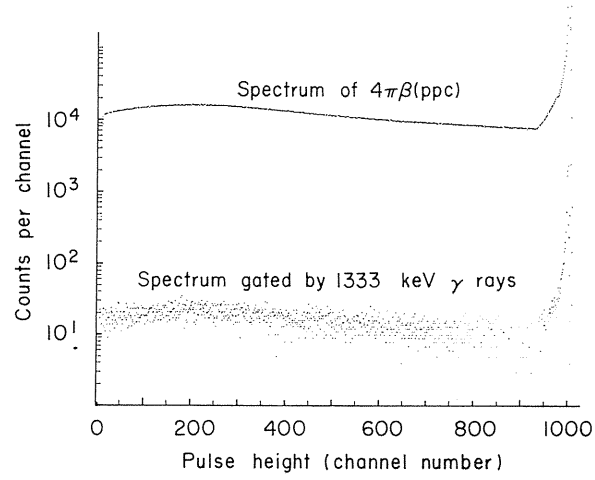

Fig. 5-1. A spectrum of ^{60}Co obtained from the $4\pi\beta$(ppc) and that gated by the 1333 keV γ-rays.

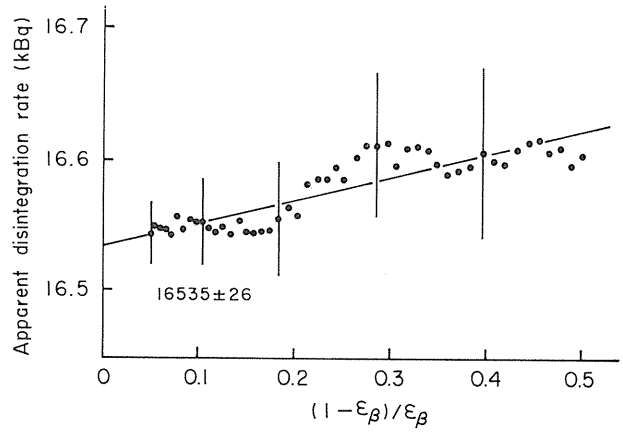

Fig. 5-2. A typical coincidence efficiency function of ^{60}Co derived by the computer discrimination method for the gate set of the 1333 keV γ-rays.

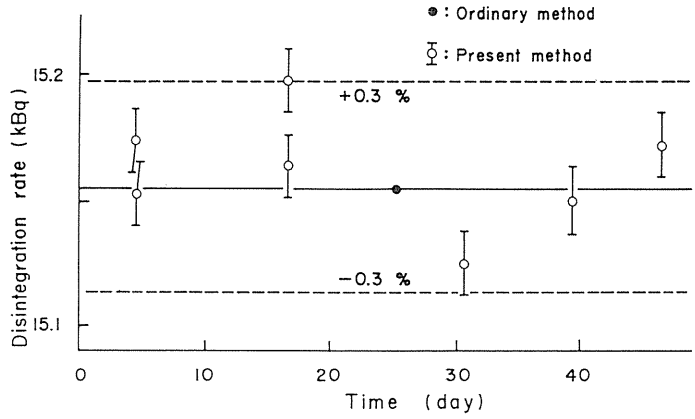

Fig. 5-3. Disintegration rates of a ^{60}Co source measured repeatedly by the present method and by ordinary method.

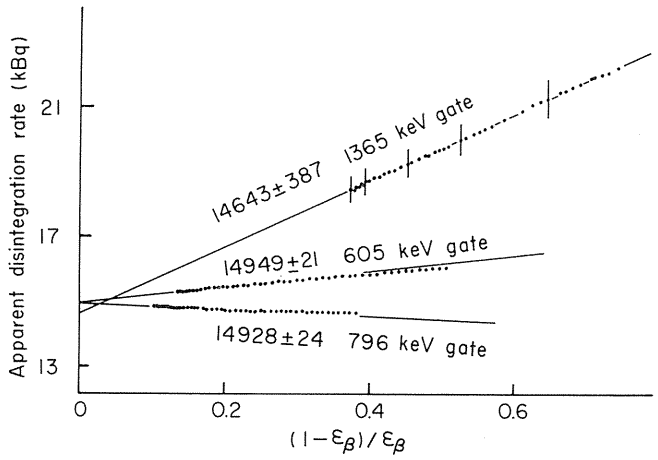

Fig. 5-4. Coincidence efficiency functions of ^{134}Cs measured by the present method. Extrapolations were carried out using data points from 0 to 0.22, 0.22 and 0.80 in the abscissa for curves obtained by the gate sets of the 605, 796 and 1365 keV γ-rays, respectively.

Table 5-1. Comparison of the disintegration rates of a ^{134}Cs source obtained from the present and the conventional methods.

	Disintegration rate (Bq)			
	4πβ(ppc)-γ(NaI) ordinary method		4πβ(ppc)-γ(HPGe) bi-dimensional method	
Gate	605 keV	796 keV	605 keV	796 keV
1	15217 ± 10	15163 ± 12	15146 ± 30	15090 ± 33
2	15150 ± 24	15193 ± 12	15249 ± 21	15161 ± 25
3	15174 ± 29	15146 ± 35	15262 ± 21	15213 ± 24
4		15192 ± 16	15200 ± 22	15185 ± 25
Mean	15204 ± 9	15180 ± 7	15224 ± 11	15172 ± 13
Mean	15190 ± 6		15202 ± 9	

two beta branches gives different results in spite of no conversion electron. Fig. 5-4 shows the coincidence efficiency functions obtained for the gate sets of the 563 and 605 keV gamma-rays, the 796 and 802 keV gamma-rays and the weak 1365 keV gamma-rays. The result for the gate set of the 1365 keV gamma-rays gave large slope and low beta-ray detection efficiency because the beta-rays with low maximum energy of 89 keV was measured related with the gamma-ray coincidence. Furthermore, the small emission probability (3%) of the 1365 keV gamma-rays introduced large uncertainty, then the use of the 1365 keV gamma-rays was impractical. On the other hand, the results in the other two cases showed high detection efficiencies and small slope because of the beta-rays with high maximum energy of

658 keV in the related beta branch. The comparison between these results and those by ordinary counting is shown in Table 5-1, and the weighted mean agreed each other similarly to the case of ^{60}Co. The measurement time by this method was about 50 min, whereas that by the ordinary method was about 12 h.

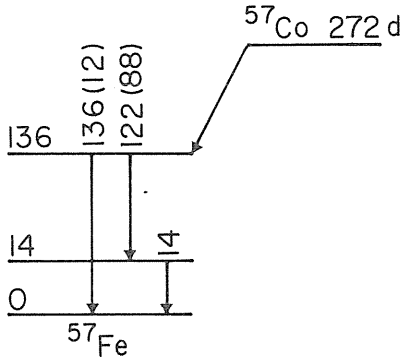

Fig. 5-5. A relevant decay scheme of ^{57}Co.

^{57}Co which decays by electron capture (EC) emits internal conversion electrons and Auger electrons/X-rays with high probability, and these radiations cannot be distinguished from those associated with EC. The decay scheme shown in Fig. 5-5 is sufficient for the view point of disintegration measurement, and it must be considered that the detection efficiency for the internal conversion electrons is not kept to be constant when the efficiency of the $4\pi\beta$(ppc) is changed. Smith and Stuart[16] proposed two-dimensional extrapolation method to resolve the above problem. Roughly describing the outline, two gates are set on the photopeaks of the 122 and 136 keV gamma-rays and coincidence counting is carried out between signals from $4\pi\beta$(ppc) and each gamma channels (n_β, $n_{\gamma 1}$, n_{c1}, $n_{\gamma 2}$, n_{c2}). The detection efficiency for the Auger electrons/X-rays is ε_c and one for the 14 keV internal conversion electrons is ε_y, then each count rate is expressed as

$$n_\beta = n_0 \sum a_i \{ \varepsilon_c + (1 - \varepsilon_c) F_i + b_i (1 - \varepsilon_c) (1 - G_i) \varepsilon_y \} \tag{5-1}$$

$$n_{\gamma 1} = n_0 a_1 b_1 (1 - G_1) \varepsilon_{\gamma 1} \tag{5-2}$$

$$n_{\gamma 2} = n_0 a_1 (1 - b_1) (1 - H_1) \varepsilon_{\gamma 2} \tag{5-3}$$

$$n_{c1} = n_{\gamma 1} \{ \varepsilon_c + (1 - \varepsilon_c) \varepsilon_y \} \tag{5-4}$$

$$n_{c2} = n_{\gamma 2} \varepsilon_c \tag{5-5}$$

where a_i is the i-th EC branching ratio, b_i is the fraction of the decay passing through the 14 keV level. The term F_i is the probability of any transition except for the 14 keV transition from the i-th branch whose events are detected by the $4\pi\beta$(ppc), and F_i can be written as a sum of a contribution G_i from a fraction b_i passing through the 14 keV level and a contribution H_i from the remainder.

The detection efficiencies of the beta counter are given for the gates of the 122 and 136 keV gamma-rays by:

$$\varepsilon_1 = \frac{n_{c1}}{n_{\gamma 1}} = \varepsilon_c + (1 - \varepsilon_c)\,\varepsilon_y \tag{5-6}$$

$$\varepsilon_2 = \frac{n_{c2}}{n_{\gamma 2}} = \varepsilon_c \tag{5-7}$$

Dividing Eq. (5-1) by Eq. (5-6) or (5-7), the following coincidence equations are obtained:

$$\frac{n_\beta}{\varepsilon_1} = n_0 \left[1 + \frac{1-\varepsilon_1}{\varepsilon_1} \cdot \frac{1}{1-\varepsilon_y} \{ \sum a_i F_i - \varepsilon_y + \varepsilon_y \sum a_i b_i (1 - G_i) \} \right] \tag{5-8}$$

$$\frac{n_\beta}{\varepsilon_2} = n_0 \left[1 + \frac{1-\varepsilon_2}{\varepsilon_2} \{ \sum a_i F_i + \sum a_i b_i (1 - G_i)\, \varepsilon_y \} \right] \tag{5-9}$$

Since ε_y changes with ε_1 and ε_2, it is difficult to extrapolate correctly. Then, the substitution of ε_y from Eqs. (5-6) and (5-7) into Eq. (5-8) gives

$$\frac{n_\beta}{\varepsilon_1} = n_0 \left[1 + \frac{1-\varepsilon_1}{\varepsilon_1} \sum a_i F_i + \left(1 - \frac{\varepsilon_2}{\varepsilon_1}\right) \{ \sum a_i F_i - 1 + \sum a_i b_i (1 - G_i) \} \right] \tag{5-10}$$

The disintegration rate n_0 can be determined by simultaneous linear extrapolation of the efficiency function as $(1-\varepsilon_1)/\varepsilon_1$ and $(1-\varepsilon_2/\varepsilon_1)$ fall to zero. The coincidence efficiency functions obeyed by Eqs. (5-8) and (5-9) are shown in Figs. 5-6 and 5-7. Fig. 5-6 shows a clear curved

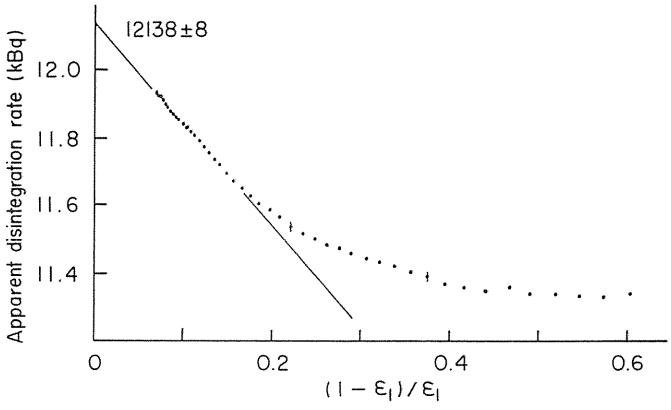

Fig. 5-6. A coincidence efficiency function of ^{57}Co derived by the computer discrimination method for the gate set of the 122 keV γ-rays.

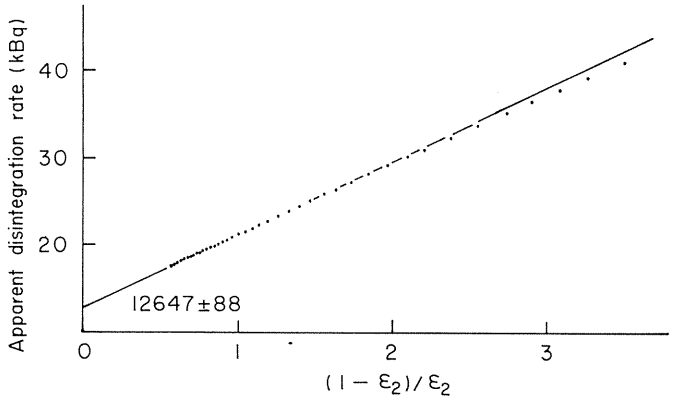

Fig. 5-7. A coincidence efficiency function of ^{57}Co derived by the computer discrimination method for the gate set of the 136 keV γ-rays.

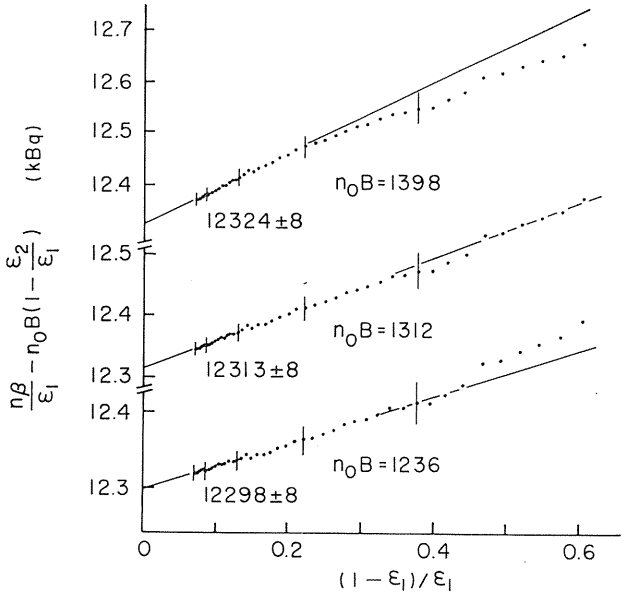

Fig. 5-8. Two dimensional extrapolation of ^{57}Co. The gates 1 and 2 were set on the peaks of the 122 and the 136 keV γ-rays, respectively.

efficiency function. Curved efficiency function is not clear in Fig. 5-7 because of large scale of longitudinal axis. Though, the dependency of the extrapolated value on the fitting region shows that the efficiency function is not straight, but curved.

Fig. 5-8 shows the result of two-dimensional extrapolation based on Eq. (5-10). In the figure the third term of right hand side in Eq. (5-10) is transferred to left hand side:

$$\frac{n_\beta}{\varepsilon_1} - (1 - \frac{\varepsilon_2}{\varepsilon_1})\, n_0 B = n_0 (1 + \frac{1 - \varepsilon_1}{\varepsilon_1} A)$$
$$A = \sum a_i F_i, \quad B = A - 1 + \sum a_i b_i (1 - G_i) \tag{5-11}$$

Therefore, constant A need not to calculate, because the slope of the linear function gives the value of A. On the other hand, calculation of constant B is not expected to give sufficient certainty, but the most probable value of n_0B which is recognised as a constant gives a linear extrapolation function in actual procedure (Fig. 5-8). The disintegration rate is determined by the extrapolation of linear function.

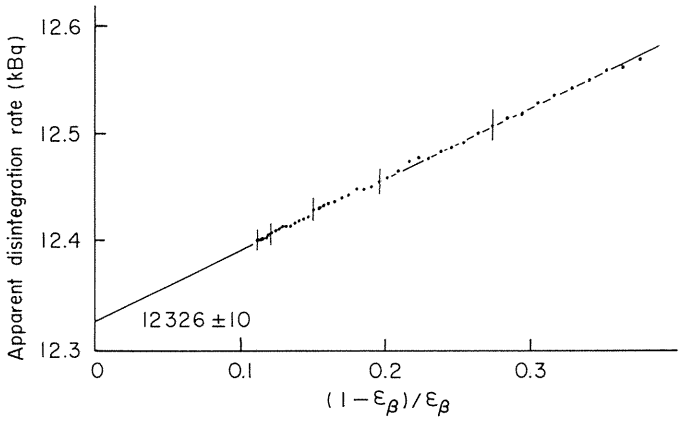

Fig. 5-9. A coincidence efficiency function of ^{57}Co derived by the computer discrimination method for the gate set of both the 122 and 136 keV γ-rays.

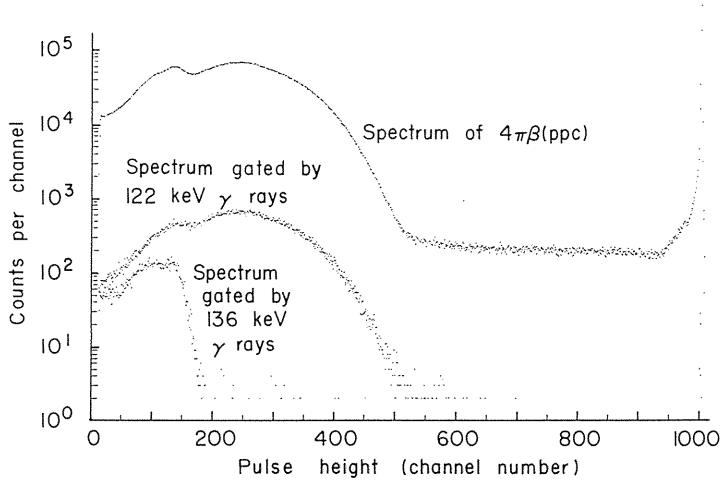

Fig. 5-10. A spectrum of ^{57}Co obtained from the $4\pi\beta$(ppc) and those gated by the 122 and the 136 keV γ-rays.

In the coincidence counting using a NaI(Tl) detector the separation of the 122 and 136 keV gamma-rays is difficult, then disintegration rate is approximately determined from the ordinary coincidence counting using the gate of both gamma-rays. Numerical analysis predicted that the disintegration rate determined by the gate set was smaller than the true by 0.1%[16], and it is consistent with the result shown in Fig. 5-9 that was measured by gate set of both gamma-rays using this system. The $4\pi\beta$(ppc) spectra of ^{57}Co obtained simply and coincident with each gate are shown in Fig. 5-10.

5. 2. *Measurement of disintegration rate of* ^{152}Eu

The multi gamma-ray emitter ^{152}Eu has well established gamma-ray emission probabilities [2,17,18], and is a preferred radionuclide for the efficiency calibration of high-resolution detectors. This radionuclide decays via β^--particle emission (27%) and electron capture (EC, 73%) accompanied by a substantial fraction of conversion electrons, which complicates activity measurement by $4\pi\beta$-γ coincidence counting.

Large $4\pi\gamma$ scintillation detectors have been used to standardise ^{152}Eu[19,20], and uncertainties are in the range 0.2 to 0.6%. $4\pi\beta$-γ spectroscopic coincidence method with an uncertainty of approximately 0.6% can also be used[21] by monitoring the single gamma spectrum and the gamma spectrum coincident with the pulses from the $4\pi\beta$-counter. Both methods have uncertainties that are affected by the decay scheme. The current studies involve the standardisation of ^{152}Eu using this system and adopting the method of two-dimensional efficiency extrapolation. The identical data were also analysed by conventional efficiency extrapolation and $4\pi\beta$-γ spectroscopic coincidence method.

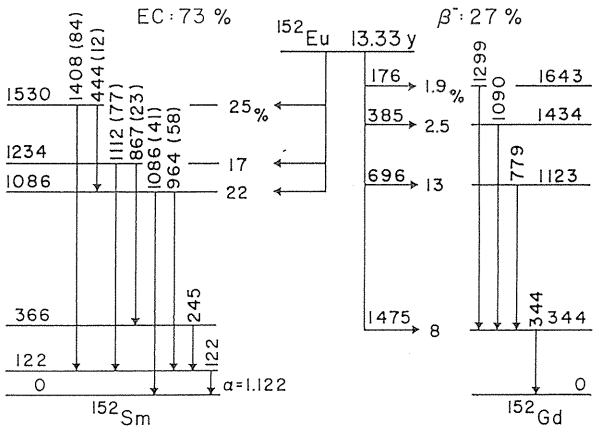

Fig. 5-11. A relevant decay scheme of ^{152}Eu.

Fig. 5-11 shows the decay scheme of ^{152}Eu without the weak transitions. Inefficiencies must remain linearly related as they increase in order for the efficiency extrapolation to be valid. However, ^{152}Eu emits a significant fraction of internal conversion electrons from the 122 keV transitions following EC decay, with variable inefficiencies that are not proportional to the measured inefficiencies. Extending Eq. (5-1), the beta-detector count rate (n_β) has to be expressed as

$$n_\beta = n_0 \Big[\sum a_i \{ \varepsilon_c + (1 - \varepsilon_c) F_i + b_i (1 - \varepsilon_c) (1 - G_i) \varepsilon_y \} + \sum d_i \{ \varepsilon_{\beta i} + (1 - \varepsilon_{\beta i}) J_i \} \Big] \tag{5-12}$$

where d_i is the i-th beta branching ratio, $\varepsilon_{\beta i}$ represents the efficiency of the $4\pi\beta$(ppc) to beta-rays and J_i is the probability of any transition from the i-th beta branch counted by the beta detector. The other notations were described in section 5.1, whereas the objective transition here changes from the 14 keV to the 122 keV.

When the gate is set to detect gamma-rays following the beta transitions, the gamma and coincidence count rates ($n_{\gamma b}$, n_{cb}) are given by:

$$n_{\gamma b} = n_0 \sum d_i m_i \varepsilon_{\gamma b} \tag{5-13}$$

$$n_{cb} = n_0 \sum d_i m_i \varepsilon_{\gamma b} \varepsilon_{\beta i} \tag{5-14}$$

where m_i represents the relative i-th branching ratio for the gamma-ray emissions. The mean beta detection efficiency (ε_β) for the above conditions is defined from Eqs. (5-13) and (5-14) as

$$\varepsilon_\beta = \frac{n_{cb}}{n_{\gamma b}} . \tag{5-15}$$

The coincidence equation is therefore:

$$\frac{n_\beta}{\varepsilon_\beta} = n_0 \Big[1 + \frac{1 - \varepsilon_\beta}{\varepsilon_\beta} \Big[1 - \sum d_i C_{bi} (1 - J_i) - \sum a_i C_c \{ 1 - F_i - b_i (1 - G_i) \varepsilon_y \} \Big] \Big] \tag{5-16}$$

where

$$C_{bi} = \frac{1 - \varepsilon_{\beta i}}{1 - \varepsilon_\beta}, \quad C_c = \frac{1 - \varepsilon_c}{1 - \varepsilon_\beta} .$$

If C_{bi}, C_c, J_i, F_i, G_i and ε_y are constant, the efficiency function given by Eq. (5-16) is linear. However, C_c is not constant if ε_β changes largely. Furthermore at high values of ε_β, ε_y may change with a small change in ε_β because of the increased detection efficiency of Auger electrons and X-rays.

When the gate is set to detect gamma-rays following EC decays (other than those associated with the 122 keV level), the gamma and coincidence count rates ($n_{\gamma e1}$, n_{ce1}) are given by:

$$n_{\gamma e1} = n_0 \sum a_i n_i \varepsilon_{\gamma e1} \tag{5-17}$$

$$n_{ce1} = n_{\gamma e1} \varepsilon_c \tag{5-18}$$

where n_i is the relative branching ratio for the gamma-ray emissions. The detection efficiency for EC decay (Auger electrons and X-rays) can be derived from Eqs. (5-17) and (5-18):

$$\varepsilon_1 = \frac{n_{ce1}}{n_{\gamma e1}} = \varepsilon_c \,. \tag{5-19}$$

Then the coincidence equation is given by

$$\frac{n_\beta}{\varepsilon_c} = n_0 \left[1 + \frac{1-\varepsilon_c}{\varepsilon_c} \left[1 - \sum d_i \, C_{di} \, (1 - J_i) - \sum a_i \{ 1 - F_i - b_i \, (1 - G_i) \, \varepsilon_y \} \right] \right] \tag{5-20}$$

where

$$C_{di} = \frac{1-\varepsilon_{\beta i}}{1-\varepsilon_c} \,.$$

If the terms C_{di}, J_i, F_i, G_i and ε_y are constant, Eq. (5-20) gives a linear function, although ε_y may change slightly with ε_c.

When the gate is set to admit gamma-rays followed by the 122 keV transitions,

$$n_{\gamma e2} = n_0 \sum a_i \, b_i \, (1 - G_i) \, \varepsilon_{\gamma e2} \tag{5-21}$$

$$n_{ce2} = n_{\gamma e2} \{ \varepsilon_c + (1 - \varepsilon_c) \, \varepsilon_y \} \tag{5-22}$$

$$\varepsilon_2 = \frac{n_{ce2}}{n_{\gamma e2}} = \varepsilon_c + (1 - \varepsilon_c) \, \varepsilon_y \tag{5-23}$$

$$\frac{n_\beta}{\varepsilon_2} = n_0 \left[1 + \frac{1-\varepsilon_2}{\varepsilon_2} \left[1 - \sum d_i \, C_{di} \, (1 - J_i) \frac{1}{1-\varepsilon_y} - \sum a_i \{ 1 - F_i - b_i \, (1 - G_i) \, \varepsilon_y \} \frac{1}{1-\varepsilon_y} \right] \right] . \tag{5-24}$$

It is very important that ε_y suffers no change with any change in the counting efficiency. Thus, the substitution of ε_y from Eq. (5-23) into Eq. (5-16) gives:

$$\frac{n_\beta}{\varepsilon_\beta} + n_0 \, D \left(1 - \frac{\varepsilon_2}{\varepsilon_\beta}\right) = n_0 \left\{ 1 + \frac{1-\varepsilon_\beta}{\varepsilon_\beta} (1 - A - B + C) \right\} , \tag{5-25}$$

where

$$A = \sum d_i \, C_{bi} \, (1 - J_i) \,, \qquad B = \sum a_i \, C_c \, (1 - F_i)$$

$$C = \sum a_i \, b_i \, (1 - G_i) \, (C_c - 1) \,, \qquad D = \sum a_i \, b_i \, (1 - G_i) \,.$$

This equation is a similar form to Eq. (5-11). Therefore, after measurements at the different efficiencies of ε_β and ε_2, the disintegration rate n_0 can be determined by simultaneous linear extrapolation of the efficiency function as $(1\text{-}\varepsilon_\beta)/\varepsilon_\beta$ and $(1\text{-}\varepsilon_2/\varepsilon_\beta)$ fall to zero.

The substitution of Eq. (5-23) into Eq. (5-20) gives

$$\frac{n_\beta}{\varepsilon_c} + n_0 D\left(1 - \frac{\varepsilon_2}{\varepsilon_c}\right) = n_0\left\{1 + \frac{1-\varepsilon_c}{\varepsilon_c}(1 - A' - B')\right\} \tag{5-26}$$

where

$$A' = \sum d_i C_{di}(1 - J_i), \quad B' = \sum a_i (1 - F_i).$$

The disintegration rate n_0 can also be obtained by two-dimensional extrapolation.

Fig. 5-12 (a) shows the efficiency function obtained with the gate set on the photopeak of the 779 keV gamma-rays (Eq. (5-16)). The linear fit to the data is considerably smaller than the extrapolation range, resulting in a large uncertainty in the disintegration rate. The efficiency functions for the 1086 and the 964 keV gamma-rays are shown in Figs. 5-12 (b) and 5-12 (c) respectively (Eqs. (5-20) and (5-24)). Extrapolated disintegration rates are shown in

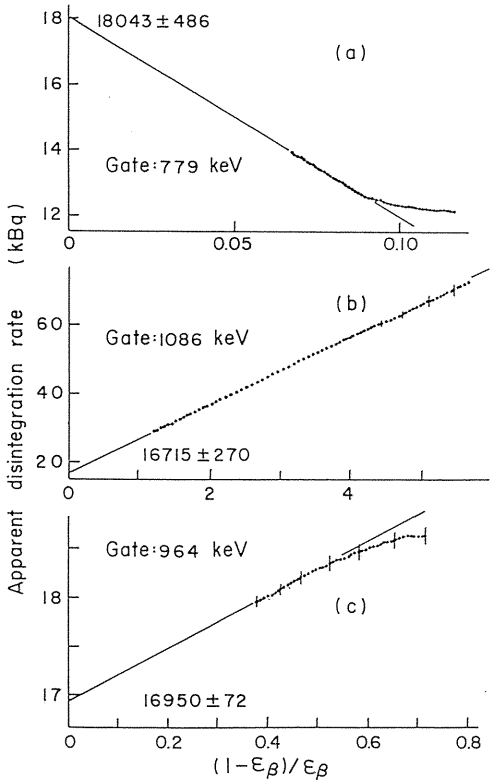

Fig. 5-12. Coincidence efficiency functions of ^{152}Eu derived by the computer discrimination method.

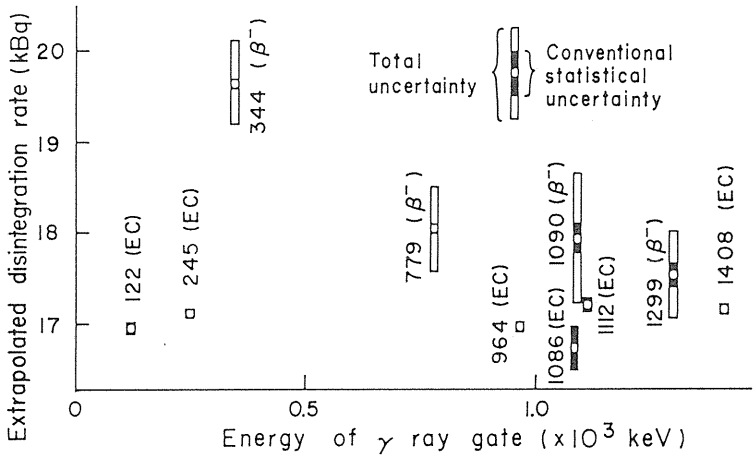

Fig. 5-13. Extrapolated disintegration rates of ^{152}Eu for various γ gates; the total uncertainty includes the standard deviation of $(1-\varepsilon_\beta)/\varepsilon_\beta$.

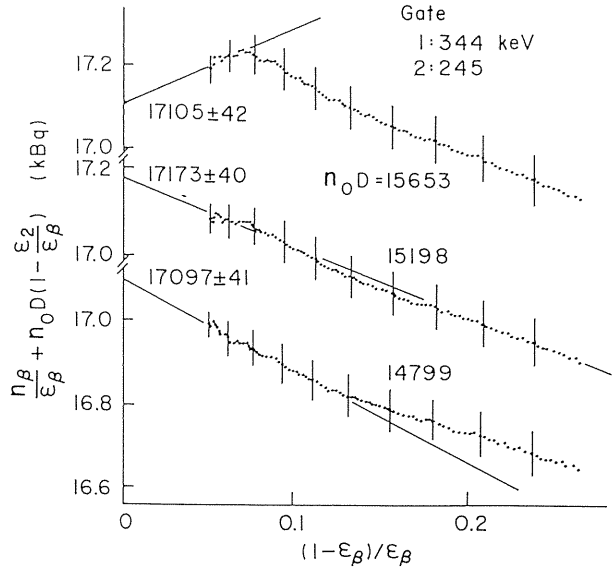

Fig. 5-14. An example of two dimensional extrapolation of ^{152}Eu. The most probable value of n_0D derived by iteration shows a linear function over extended range.

Fig. 5-13 for ten principal gamma-rays. Although the standard deviation is usually small for the conventional extrapolation procedure, all gamma count rates were low and resulted in relatively large statistical uncertainties.

While it is difficult to calculate the constant D from Eq. (5-25) when working with ^{152}Eu, it is only necessary to determine n_0D and the reliability of the data can be estimated from the efficiency function. Fig. 5-14 shows an example of two-dimensional extrapolation

when the gates are set for the 344 and 245 keV gamma-rays (Eq. (5-25)). Small and large values of n_0D result in curved efficiency functions, even though the results from these data suggest a reasonably accurate disintegration rate. The most probable value of n_0D, however, can be derived by iteration, and leads to a linear function over an extended range.

When the gates are set on the 1408 keV gamma-rays (that is followed by the 122 keV transition) and the 1086 keV gamma-ray (that is not followed by the 122 keV transition), the resulting efficiency function represented by Eq. (5-26) is produced as shown in Fig. 5-15. Changes in the value of n_0D resulted in no clear difference because of the extended longitudinal scale, although the minimum of variance generated the most appropriate n_0D to calculate the disintegration rate. An equation similar to Eq. (5-25) or (5-26) can be derived with ε_β or ε_c replaced by ε_2. An example is Fig. 5-16 where ε_β is replaced by ε_2 for the same gamma gates as shown in Fig. 5-14. However, as shown in Fig. 5-12 (c), the fitting range is smaller than before because the value of ε_y hardly decreases in spite of the change of ε_c.

There are about 30 combinations of gates that can be used to obtain the counts with adequate intensities. Table 5-2 lists a selection of these combinations in which "conventional σn_0" refers to the sum of uncertainties due to the fitting procedure and the counting statistics,

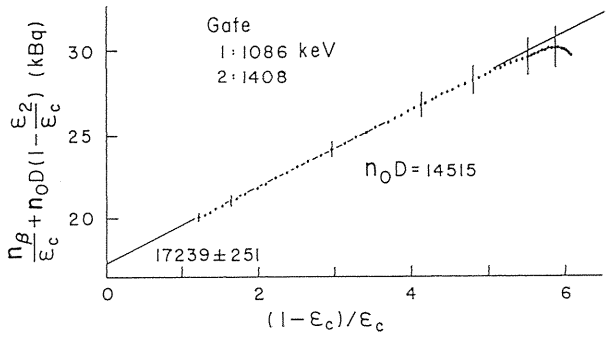

Fig. 5-15. An example of two dimensional extrapolation of ^{152}Eu in which the gates were set on the γ-rays following electron capture decay. The gradient is smaller than that of Fig. 5-12(b).

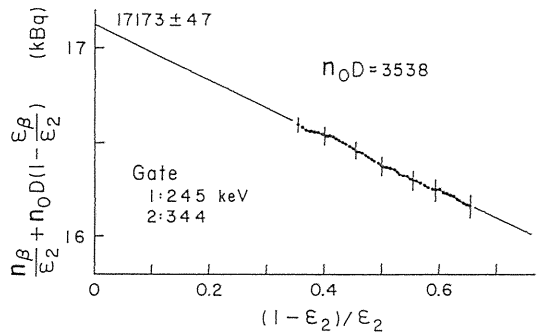

Fig. 5-16. An example of two dimensional extrapolation of ^{152}Eu in which $(1-\varepsilon_2)/\varepsilon_2$ is chosen as the horizontal axis.

Table 5-2. Selected results of two dimensional extrapolation of ^{152}Eu. "all σn_0" includes the uncertainty due to the efficiency variable.

Gate (keV)		Fitting range		n_0 (Bq)	σn_0 (Bq)	
1	2				Conventional	All
245	344	0.36	0.80	17178	46	47
344	245	0.05	0.26	17173	40	41
1408	1086	0.38	0.60	16792	86	113
1086	1408	1.22	5.00	17239	283	284
1408	779	0.37	0.85	17218	71	73
779	1408	0.07	0.35	17221	61	63
964	122	0.38	0.80	16995	82	139
122	964	1.19	5.00	17079	62	68

Table 5-3. Comparison of the disintegration rates of a ^{152}Eu source obtained with various analytical methods when referred to a common reference time. Results for the two dimensional extrapolation are the mean of four results (344 keV −245, 964, 1112, 1408 keV).

Method	Disintegration rate (Bq)			
	Elapsed time (d)			Mean
	0	22	92	
Conventional 1408 keV	14416±62	14525±65	14419±40	14453±33
Two-dimensional 344 - γ_{EC}	14443±30	14469±31	14443±19	14452±16
$4\pi\beta$-γ spectroscopic coincidence	14625±172	14218±75	14195±74	14346±67
Spectrometrical analysis	14375±140	14535±140	14340±140	14417±81

and "all σn_0" takes account of the uncertainty contribution of the efficiency parameters shown along the X-axis in addition to the above sum. The results obtained for the 1086 keV gamma-rays were particularly uncertain because of the very narrow gate set to avoid the contribution from the 1090 keV gamma-rays.

Conventional efficiency extrapolation resulted in large uncertainties (Figs. 5-12 (a) and 5-13) when the gates were used to count the gamma-rays following β^- decay because of the small fitting ranges. The largest deviations occurred for gate set involving high energy β^- emissions because the discrimination against these particles also caused an uncertain decrease in the detection efficiency for the conversion electrons. However, the gates for the gamma-rays following EC decay appeared to give reasonably good results, although the scatter of these results was rather large except for the gate set on the 1408 keV gamma-rays. It should be noted that none of the Compton background following beta-decay affected the result for the 1408 keV gamma-rays.

There are many combinations of two-gamma gating when using two-dimensional extrapolation. The intensities, statistical stabilities and widths of fitting range must be considered when selecting the gate. Hence, one gate should include only the 344 keV gamma-rays, while the other gate for the gamma-rays accompanied by conversion electrons can be chosen from the 245, 964, 1112 or 1408 keV photopeak.

The validity of these results was confirmed by analysing the identical data by the $4\pi\beta$-γ spectroscopic coincidence method[21] and by spectrometric analysis. The single and coincidence gamma-ray spectra were obtained from the stored data, while the spectrometric analysis was undertaken by comparing the gamma-ray detection efficiency function of ^{152}Eu with that of ^{60}Co as determined by coincidence counting. The results for the four different methods are listed in Table 5-3 and are in good agreement. Although conventional efficiency extrapolation has not been used to standardise ^{152}Eu so far, reasonably satisfactory data were obtained using computer discrimination[5] with the gate set to admit only the 1408 keV gamma-rays. The measurements based on independent data were less certain because of the small ratio between the extrapolation distance and fitting range. On the other hand, standardisation by two-dimensional efficiency extrapolation gave more satisfactory results, with the gate set on the 344 keV gamma-rays following beta-decay and the gamma-rays that are followed by the 122 keV transition. The ratio of the fitting range to the extrapolation distance was about five. It can be assumed that good results will also be obtained when using the conventional discrimination method without computer control and manipulation.

5. 3. *Measurement of disintegration rate of* ^{133}Ba

The multi gamma-ray emitter ^{133}Ba has also well established gamma-ray emission probabilities[1,3,22], and is a preferred radionuclide for the efficiency calibration of high resolution detectors at several hundreds keV. There is, however, a problem in disintegration rate measurement by the $4\pi\beta$-γ coincidence counting, since this nuclide emits a large amount of internal conversion electrons with low energies. Actually, the results obtained from the international comparison of ^{133}Ba[23] suggested that the extrapolated disintegration rate depended on the gamma-gate setting. Therefore, the coincidence counting has been carried out by gate set on the photopeaks above, at least, 200 keV.

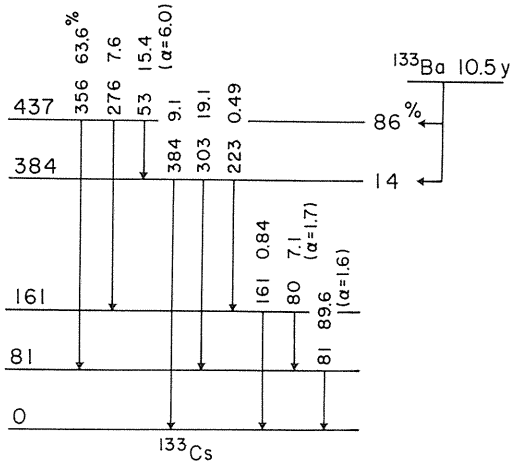

Fig. 5-17. A relevant decay scheme of ^{133}Ba.

Fig. 5-17 shows the decay scheme of ^{133}Ba in which the transitions of the 80 and 81 keV are largely internally-converted. The situation is further complicated by the fact that the 53 keV transition from the 437 keV to the 384 keV level is also internally-converted. Considering the above condition, the count rate of the beta detector (n_β) has to be expressed as

$$\begin{aligned} n_\beta = {} & n_0\,\varepsilon_c + n_0\,(1-\varepsilon_c)\,a_1\Big[\,F_1 + (1-b_1-c_1)\,(1-G_{11})\,\varepsilon_{y1} \\ & + b_1\,(1-G_{12})\,(\varepsilon_{y1}+\varepsilon_{y2}-\varepsilon_{y1}\,\varepsilon_{y2}) + c_1\,(1-G_{13}) \\ & \times\{\,\varepsilon_{y3} + (1-\varepsilon_{y3})\,b_2\,(\varepsilon_{y1}+\varepsilon_{y2}-\varepsilon_{y1}\,\varepsilon_{y2})\,\}\Big] \\ & + n_0\,(1-\varepsilon_c)\,a_2\Big[\,F_2 + b_2\,(1-G_{22})\,(\varepsilon_{y1}+\varepsilon_{y2}-\varepsilon_{y1}\,\varepsilon_{y2})\Big] \end{aligned} \tag{5-27}$$

where the notation is the same as in the case of ^{57}Co, the first of the double suffixes indicates the EC branch and the second number shows the 81, 80 or 53 keV transitions, and ε_{yi} is the detection efficiency for i-th transition with internal conversions.

Considering a simple approximation that $G_{ij} = G$ and $\varepsilon_{y1} = \varepsilon_{y2} = \varepsilon_y$, Eq. (5-27) is

$$\begin{aligned} n_\beta = {} & n_0\,\varepsilon_c + n_0\,(1-\varepsilon_c)\,(a_1\,F_1 + a_2\,F_2) \\ & + n_0\,a_1\,(1-\varepsilon_c)\,(1-G)\Big[\,(1-b_1-c_1)\,\varepsilon_y \\ & + b_1\,\varepsilon_y\,(2-\varepsilon_y) + c_1\{\,\varepsilon_{y3} + (1-\varepsilon_{y3})\,b_2\,\varepsilon_y\,(2-\varepsilon_y)\,\}\Big] \\ & + n_0\,a_2\,(1-\varepsilon_c)\,(1-G)\,\varepsilon_y\,(2-\varepsilon_y)\,. \end{aligned} \tag{5-28}$$

When the gamma gate is set on one of the photopeaks of the 384, 356, 303, 276 or 80 plus 81 keV gamma-rays, the ordinary coincidence equation is obtained. A typical equation in the case of gate set on the 384 keV gamma-rays is following:

$$\begin{aligned} \frac{n_\beta}{\varepsilon_1} = {} & n_0 + n_0\frac{1-\varepsilon_1}{\varepsilon_1}\cdot\frac{1}{(a_1\,c_1+a_2)-a_1\,c_1\,\varepsilon_{y3}}\Big[-a_1\,c_1\,\varepsilon_{y3} \\ & + (a_1\,c_1+a_2)\,(a_1\,F_1+a_2\,F_2) + a_1\,(a_1\,c_1+a_2)\,(1-G) \\ & \times\{\,(1-b_1-c_1)\,\varepsilon_y + b_1\,\varepsilon_y\,(2-\varepsilon_y) + c_1\,\varepsilon_{y3} + c_1\,(1-\varepsilon_{y3})\,b_2\,\varepsilon_y \\ & \times(2-\varepsilon_y)\,\} + a_2\,(a_1\,c_1+a_2)\,(1-G)\,\varepsilon_y\,(2-\varepsilon_y)\Big]\,. \end{aligned} \tag{5-29}$$

If ε_y and ε_{y3} are constant for changing ε_1, Eq. (5-29) is approximated to be linear. Making the change in ε_1 without changing ε_{y3} can be realised only by the discrimination of L Auger electrons in the spectrum from the beta counter shown in Fig. 5-18. Therefore, the region of linear fitting is shorter than that of extrapolation, and it is difficult to extrapolate even

by the computer discrimination method. All results gave the similar tendency regardless of the selection of gamma gate; therefore, an example obtained by gate set of the 356 keV gamma-rays is shown in Fig. 5-19.

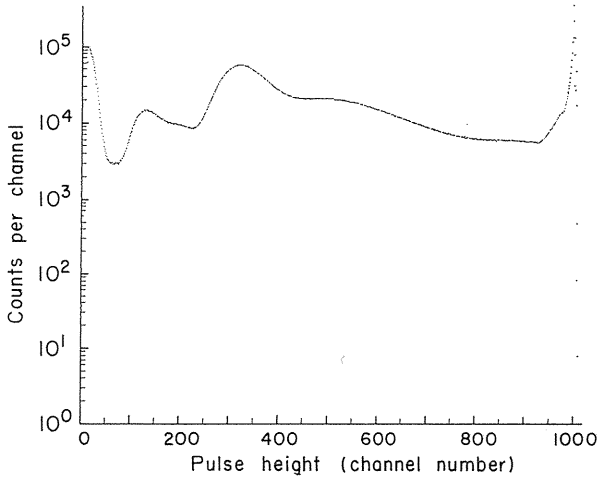

Fig. 5-18. A spectrum of ^{133}Ba obtained from the $4\pi\beta$(ppc). Three peaks correspond to L auger electrons, K conversion electrons for 53 keV and those for 80 and 81 keV transitions.

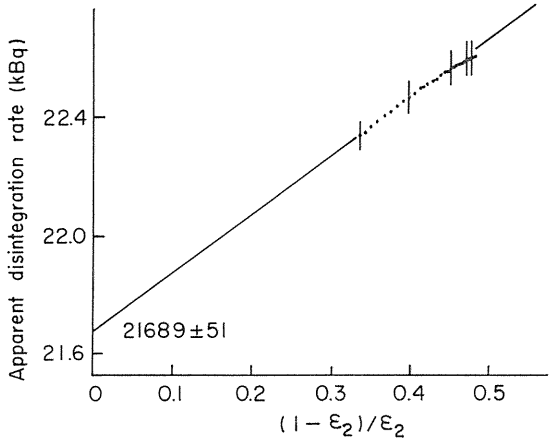

Fig. 5-19. A coincidence efficiency function of ^{133}Ba derived by the computer discrimination method for the gate set of the 356 keV γ-rays.

The reason why the data deviated from a linear line was that internal conversion electrons of the 53 keV transition (about 17 keV) were discriminated to change ε_{y3} by raising discrimination level. Then, the similar two-dimensional extrapolation method to that for ^{152}Eu

was applied to the determination of ε_{y3}. The following is described in the case of gate set on the photopeaks of the 384 and the 356 keV gamma-rays. The following equations are obtained from count rates of gamma and coincidence:

$$\frac{n_c(384)}{n_\gamma(384)} = \varepsilon_c + \frac{a_1 c_1 (1-\varepsilon_c)}{a_1 c_1 + a_2} \varepsilon_{y3} \equiv \varepsilon_1 \tag{5-30}$$

$$\frac{n_c(356)}{n_\gamma(356)} = \varepsilon_c + (1-\varepsilon_c)\,\varepsilon_y \equiv \varepsilon_2\,. \tag{5-31}$$

ε_{y3} obtained from these equations is substituted to Eq. (5-29), then

$$\frac{n_\beta}{\varepsilon_1} - \left(1 - \frac{\varepsilon_2}{\varepsilon_1}\right) \frac{n_0 K_2}{1-\varepsilon_y} = n_0 \left\{ 1 + \frac{1-\varepsilon_1}{\varepsilon_1} \left(K_1 + \frac{K_2}{1-\varepsilon_y}\right) \right\} \tag{5-32}$$

$$K_1 = 1 - (a_1 c_1 + a_2)(1-G) + (a_1 c_1 + a_2)(1-G)\, b_2\, \varepsilon_y (2-\varepsilon_y)$$

$$\begin{aligned} K_2 = {} & -(a_1 c_1 + a_2)(1 - a_1 F_1 - a_2 F_2) + a_1 (1-G)(1 - b_1 - c_1)\,\varepsilon_y \\ & + a_1 b_1 (a_1 c_1 + a_2)(1-G)\,\varepsilon_y (2-\varepsilon_y) \\ & + (a_1 c_1 + a_2)^2 (1-G) + a_1 c_1 b_2 (a_1 c_1 + a_2)(1-G)\,\varepsilon_y (2-\varepsilon_y) \\ & - (a_1 c_1 + a_2)^2 b_2\, \varepsilon_y (2-\varepsilon_y) + a_2 (1-G)(a_1 c_1 + a_2)\,\varepsilon_y (2-\varepsilon_y)\,. \end{aligned}$$

The result measured in this combination gave wide region for linear fitting shown in Fig. 5-20, although the standard deviation of final result was relatively large because of low intensity of the 384 keV gamma-rays.

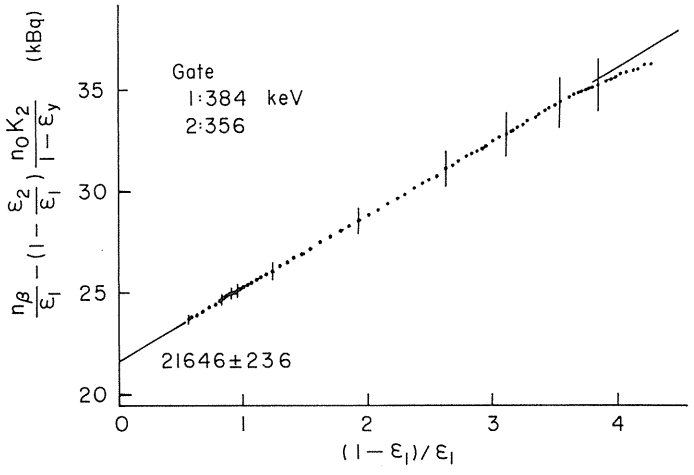

Fig. 5-20. An example of two dimensional extrapolation of ^{133}Ba.

Table 5-4. Results of ^{133}Ba obtained from the two dimensional extrapolation in all combinations of γ gates. The upper values show fitting range and the lower extrapolated disintegration rates (Bq). The symbols o and x show suitable and unsuitable combination from consideration of analytical calculation.

γ ray (keV)		Y axis (gate 2)				
		384	356	303	276	81
X axis (gate 1)	384		o 0.58~3.50 15061±85	x 0.58~0.90 15187±119	o 0.58~3.00 15298±116	o 0.58~3.50 15061±86
	356	o 0.33~0.55 15036±21		o 0.33~0.53 15101±21	x 0.33~0.54 16398±228	o 0.33~0.52 14998±39
	303	x 0.17~0.23 15202±20	o 0.17~0.40 15098±25		o 0.17~0.40 15357±50	o 0.17~0.40 15052±23
	276	o 0.18~0.28 15294±31	x 0.18~0.26 16468±123	o 0.18~0.26 15357±34		o 0.18~0.26 14345±89
	81	o 0.98~3.00 15047±51	o 0.98~3.00 15057±73	o 0.98~3.00 15082±48	o 0.98~3.00 14651±189	

Table 5-4 shows the results obtained from various combinations, where symbols, o and x, in the table indicate suitable and unsuitable combination, respectively, judging from the calculated equation. The values in column show the region capable of fitting linearly and the extrapolated disintegration rate with the standard deviation. Among the results excluding those with the symbol x, the values using the gate set on the 276 keV gamma-rays differed from others. The Compton components of high-energy gamma-rays are largely contained under the photopeak of the 276 keV gamma-rays, then it is incorrect to assume that the coincidences with the 276 keV gamma-rays would not be influenced by the conversion electrons of the 53 keV transition. Judging from the results, five combinations, 384-356, 384-81, 81-384, 81-356 and 81-303, are suitable for practical measurement.

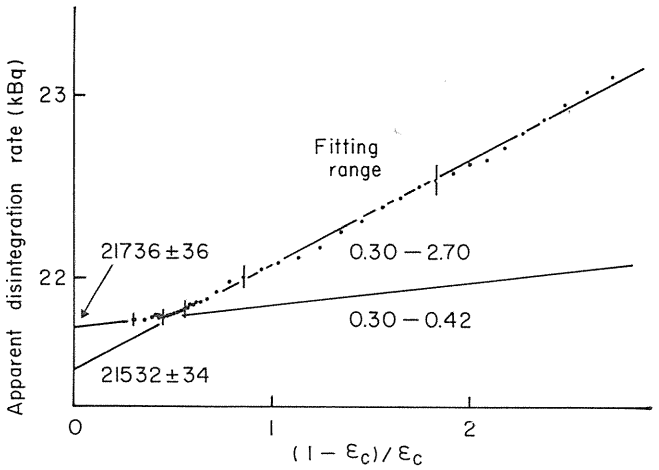

Fig. 5-21. A coincidence efficiency function of ^{133}Ba derived by the computer discrimination method for the gate set of the γ-rays from the 276 to the 384 keV.

When a wide gate was set on the peaks from the 276 to the 384 keV gamma-rays like the case of a NaI(Tl) scintillation detector[23], a small bend in the efficiency function was seen at about 0.5 of $(1-\varepsilon_\beta)/\varepsilon_\beta$ as shown in Fig. 5-21. It may be difficult to recognise the bend on the data measured by the other methods without the computer discrimination method. The fitting using the data points between 0.3 and 0.42 of $(1-\varepsilon_\beta)/\varepsilon_\beta$ gave the result to agree well with that by two-dimensional extrapolation, but the fitting using the data points between 0.3 and 2.7 gave considerably smaller value. When the gate was set on energy region from the 70 to 400 keV, this tendency was remarkable. However, the result obtained from the fitting of the narrow region agreed with that from the two-dimensional extrapolation. The fitting using only the data with high efficiencies means the pulse height discrimination of L Auger electrons; therefore, this satisfies the condition to determine n_0 in Eq. (5-29).

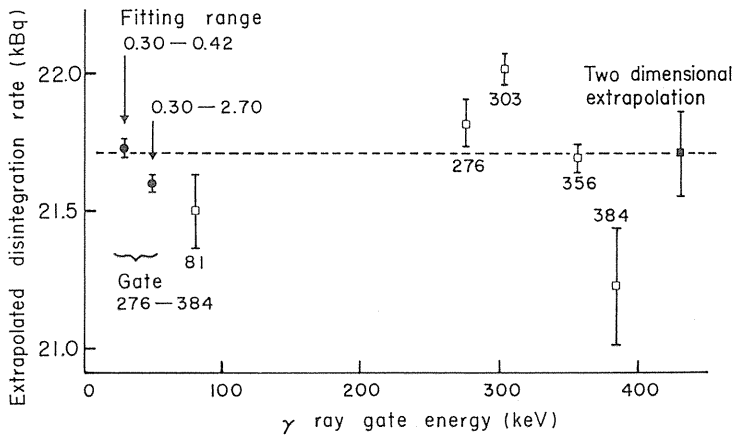

Fig. 5-22. Extrapolated disintegration rates of a ^{133}Ba source obtained from the computer discrimination method for various γ gate sets and two dimensional extrapolation.

Fig. 5-22 shows the results by two-dimensional and conventional extrapolations. The gate set on a peak of single gamma-rays in conventional coincidence counting gave narrow fitting region, then only the computer discrimination method gave these results. The results measured for gate set on the 276 and the 303 keV gamma-rays which gave negative slope of efficiency function were larger than the average and the other results obtained from that with positive slope were smaller. Besides, the fact that result for the 276 keV gamma-rays considerably differed from the other values caused the scattering of the results obtained from the combinations using the gate set of the 276 keV gamma-rays in two-dimensional extrapolation.

For the measurement of coincidence efficiency function of ^{133}Ba by the conventional extrapolation method, the computer discrimination method must be used on the gate set of the energy region from the 70 to 400 keV or from the 250 to 400 keV, otherwise narrow fitting region causes large uncertainty in final result or the fitting using ordinary wide region gives systematically small value by about 0.5%. This is the main reason that in the measurement of gamma-ray emission probability by Schotzig et al.[1] the total intensity to transit to the ground state of ^{133}Cs is larger than the total disintegration rate of ^{133}Ba by about 1.2% when the new data of conversion coefficients[24] is used. If the disintegration rate was larger than its

value by 0.5% estimated from the present measurement, then the difference was only 0.4%. On the other hand, five combinations in two-dimensional extrapolation, 384-356, 384-81, 81-384, 81-356 and 81-303, give the fitting region more than two times of extrapolation region, and good result is probably obtained even by the method without the computer discrimination.

5. 4. *Measurement of the emission probabilities for the 1099 and 1292 keV gamma-rays of* ^{59}Fe

For the demonstration of the effectiveness of our method, the emission probabilities for the principal gamma-rays of ^{59}Fe were measured. Considering that the beta-ray branch to the ground state of ^{59}Co is only 0.18%[25] and that the intensity of the 1481 keV gamma-rays is less than 0.1%, the sum of the intensities for the 1099 and the 1292 keV gamma-rays is estimated to be about 99.7%. However, the reported uncertainties of the emission probabilities are from 2 to 3%.

Since ^{59}Fe is a nuclide having relatively simple decay, the disintegration rate was measured by the method described in section 5.1 and the mean value of the results obtained

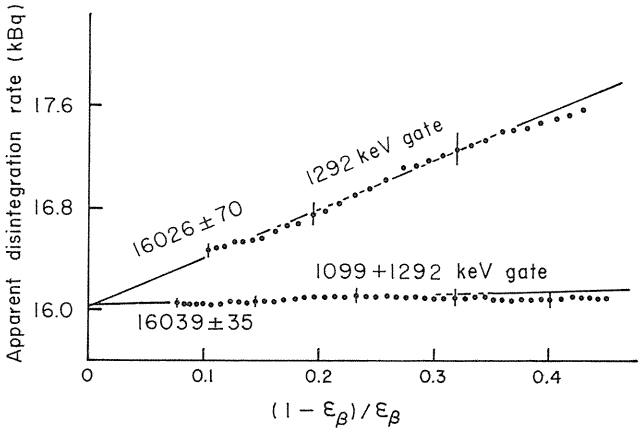

Fig. 5-23. Coincidence efficiency functions of ^{59}Fe derived by the computer discrimination method of the gate sets of the 1292 keV γ-rays and both the 1099 and the 1292 keV γ-rays.

Table 5-5. Emission probabilities for the principal γ-rays of ^{59}Fe.

Run number	Emission probabilities ($\times10^{-2}$)				
	142.6	192.4	335.0	1099.2	1291.6
1-(1)	0.929±0.020	2.836±0.040	0.258±0.020	56.47±0.38	42.82±0.31
1-(2)	0.940±0.020	2.821±0.039	0.259±0.019	56.62±0.37	42.73±0.30
2	0.962±0.020	2.835±0.037	0.246±0.023	56.56±0.38	43.20±0.31
3	0.987±0.024	2.898±0.038	0.284±0.024	56.92±0.37	43.32±0.30
Mean	0.955±0.011	2.848±0.019	0.262±0.009	56.65±0.19	43.02±0.15
Legrand et al. (27)	0.98±0.04	2.95±0.08	0.24±0.04	55.5±1.7	44.1±1.2
Pancholi et al. (28)	1.02±0.04	3.08±0.10	0.27±0.01	56.5±1.5	43.2±1.1

from gate set on the photopeaks of the 1099 and the 1292 keV gamma-rays (Fig. 5-23) was adopted as the disintegration rate. The presence of ^{55}Fe which had the possibility to be contained in ^{59}Fe as an impurity was examined carefully by the method described before[26], but the amount was less than 0.1% at that time. The results are summarised in Table 5-5 where the uncertainties are again expressed at the level of one standard deviation. The gamma-ray detection efficiency function described in section 4.2 was measured with ^{46}Sc, ^{60}Co, ^{134}Cs and ^{152}Eu at each of three runs for ^{59}Fe. Two ^{59}Fe sources at first run and one source at the other runs were measured. The reference values[27,28], although not recent, are still used by evaluators (see e.g. NCRP report No. 58 2nd edition[29]). The fact that the sum of the intensities for the 1099 and the 1292 keV gamma-rays is almost equal to unity (0.9967 ± 0.0024) shows that the values and the method are reasonable. However, the results for low-energy gamma-rays are uncertain, because only ^{152}Eu was used as calibration source at low energy region.

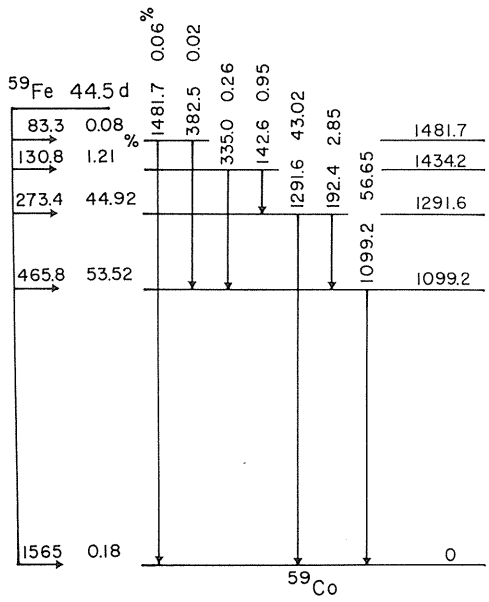

Fig. 5-24. A decay scheme for ^{59}Fe calculated from the present data for emission probabilities of the principal γ-rays.

A tentative decay scheme can be calculated for ^{59}Fe on the basis of this result and the results by Pancholi et al.[28] for the other gamma-rays and the resulting decay scheme is shown in Fig. 5-24. Considering that the sum of all beta branches except for the branch to the ground state is 0.9973 ± 0.0022 and the beta branch to the ground state is reported to be 0.0018 ± 0.0004[24], these results are satisfactory. Therefore, it is reasonable that the emission probabilities for the 1099 and the 1292 keV gamma-rays are 0.5665 ± 0.0019 and 0.4302 ± 0.0015, respectively.

5. 5. Measurement of the emission probability for the 1077 keV gamma-rays of ^{86}Rb

^{59}Fe described in the previous section scarcely decays to the ground state, and the gamma-ray emission probability for such nuclide can be determined from the relative gamma-ray intensity without measurement of disintegration rate, because the beta-branching ratios are calculated from the amount of gamma transition at each level. However, when a nuclide decays directly to the ground state, the relative beta-branching ratio in addition to the relative gamma-ray intensity is required for the determination of gamma-ray emission probability. The uncertainty in beta-branching ratio is usually large and affects the determination of gamma-ray emission probability. Therefore, the emission probability must be determined from the measurements of disintegration rate and gamma-rays. Usefulness of this apparatus for these measurements was shown in section 5.4 for ^{59}Fe as an example. In this section the result for ^{86}Rb which has large beta branch to the ground state is shown.

^{86}Rb transits directly to the ground state of ^{86}Sr with probability of about 0.9 after emission of beta-rays with maximum energy of 1780 keV. The 1077 keV gamma-rays with the emission probability of about 0.1 are emitted following the emission of beta-rays with maximum energy of 700 keV. The coincidence efficiency function of ^{86}Rb was measured by gate set on the photopeak of the 1077 keV gamma-rays to determine the disintegration rate. Fig. 5-25 shows an example of the results and there is a problem to choose linear function or polynomial one for fitting. Two kinds of fitting shown in the figure are linear fitting using narrow region and third-order polynomial fitting (without a second-order term)[30] using wide region.

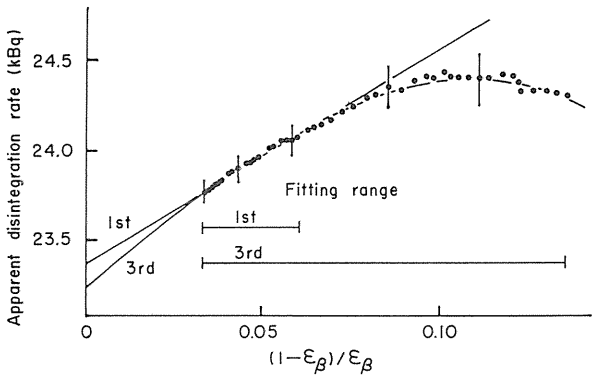

Fig. 5-25. An example of coincidence efficiency function of ^{86}Rb derived by the computer discrimination method for the gate set of the 1077 keV γ-rays. The detail is shown in the text.

In the linear fitting the extrapolated value increased with the extension of upper limit of fitting region, but did not change in the third-order polynomial fitting. The extrapolation by second-order polynomial fitting gave extremely small disintegration rate and also the degree of fitting was visually not good (not shown in the figure). These results proved correctness of the previous report[30] to recommend the third-order polynomial function without second-order term for curved efficiency function. Table 5-6 shows the emission probabilities calculated from the disintegration rates obtained by two kinds of extrapolation.

Table 5-6. Emission probability for the 1077 keV γ-rays of ^{86}Rb. The first two runs have been carried out using the HPGe detector with relative detection efficiency of 14% and the others using that with relative detection efficiency of 23%.

Run	Emission probability ($\times 10^{-2}$)		Fitting range		ε_γ ($\times 10^{-3}$)
	1st	3rd	1st	3rd	
1	8.826±0.061	8.906±0.061	0.035~0.11	0.035~0.13	1.5711±0.0089
2	8.805±0.058	8.857±0.059	0.045~0.080	0.045~0.14	1.5688±0.0088
3	8.864±0.051	8.891±0.052	0.035~0.065	0.035~0.13	1.7615±0.0096
4	8.844±0.056	8.882±0.056	0.030~0.050	0.030~0.11	1.7576±0.0095
Mean	8.835±0.028	8.884±0.029			

Table 5-7. Emission probability of the 1077 keV γ-rays of ^{86}Rb compared with published results.

Author	Emission Probability ($\times 10^{-2}$)
Campion et al. (31)	8.66 ± 0.15
Brandhorst et al. (32)	8.79 ± 0.09
Gupta et al. (33)	8.9 ± 0.3
Present work	8.884 ± 0.029

Four times of measurements were carried out and the gamma-ray detection efficiency function described in section 4.2 was measured at each run using sources, ^{60}Co, ^{134}Cs and ^{152}Eu. Three sources of ^{86}Rb of which disintegration rates were determined from two measurements were used for each run. The emission probability shown in the table is mean of three sources and the fitting region is a typical mean value. The emission probabilities obtained from the linear fitting are smaller than those obtained from the third-order fitting by 0.2% to 0.9%. Particularly, when wide fitting region was used in the linear fitting, the difference in the final result was large even though good fitting was obtained. Then, the adopted result was obtained from the extrapolation by using the third-order fitting, because it filled the requirement that the function changed linearly near unity of detection efficiency and also because it fitted well with the experimental points. The former and the latter two runs were carried out using the HPGe detectors with relative efficiencies of 14% and 23%, respectively, but there was no difference.

Table 5-7 lists various measurements of the emission probability for the 1077 keV gamma-rays, including the result from the present work. Campion et al.[31] measured the gamma-ray intensity by ionisation chamber, Brandhorst et al.[32] determined the disintegration rate by use of a proportional counter and the result by Gupta et al.[33] had large uncertainty. Considering these points, the present value agrees with other works, but only it has an improved certainty.

5. 6. *Measurement of the emission probabilities for the 497, 557 and 610 keV gamma-rays of* ^{103}Ru

A large part of the transition from ^{103}Ru goes through the 40 keV metastable level of ^{103}Rh that has half-life of 56 min and the transition from it has a large internal conversion coefficient. Kocher[34] evaluated that the beta branch to the 40 keV level was 6.4%, the decay scheme by Harmatz[35] showed that beta branch of 3.5% went to the 40 keV or ground level and Frenne et al.[36] evaluated no beta transition to the 40 keV level and only 0.87% of beta transition to the ground level. These variations depend on the large internal conversion coefficient for the 40 keV transition and no accurate data concerned with beta-ray measurement; therefore, the emission probability of gamma-rays could not be determined from the relative gamma-ray intensity. The result of beta-ray measurement by Pettersson et a1.[37] was only one significant data before 1982, but since then the value measured using beta-ray spectrometer by Ohshima et al.[38] has been treated as a leading data. On the other hand, relative gamma-ray intensities by Macias et al.[39] has also been fundamental data in evaluation.

It is difficult to determine the disintegration rate in the case that the internal conversion electrons are emitted from the metastable state. The count rate of the $4\pi\beta$ counter at detection efficiency of unity becomes larger than the disintegration rate by emission probability of the internal conversion electrons, since it detects both beta-ray and conversion electron per decay. If the decay scheme is known, the correction is easy. However, when the beta branch to the ground state is not clear like this case, the emission probability for the internal conversion electrons is not clearly determined. Then, the disintegration rate is determined from the assumed decay scheme and the new decay scheme is calculated from the gamma-ray emission probabilities determined from the disintegration rate and gamma-ray measurement. The result must agree with the assumed one; therefore, disagreement requires repeated calculation till convergence.

When the gate is set on the photopeak of the 497 keV gamma-rays to obtain the coincidence efficiency function of ^{103}Ru, the detection efficiency for beta-rays with maximum energy of the 226 keV becomes standard efficiency. On the other hand, gate setting on the photopeak of the 557 or the 610 keV gamma-rays brings the efficiency of beta-rays with maximum energy of the 113 keV to be the standard. In the latter gate, low-energy of beta-rays and weak intensity of gamma-rays introduced uncertain result, then only the former gate

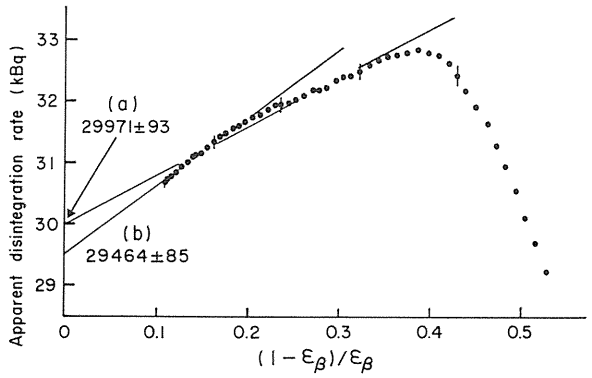

Fig. 5-26. An example of coincidence efficiency function of ^{103}Ru derived by the computer discrimination method for the gate set of the 497 keV γ-rays. The linear extrapolations (a) and (b) are obtained from the fitting using the data in narrow and wide region, respectively.

was used. Fig. 5-26 shows an example of the coincidence efficiency function for ^{103}Ru. It is an important problem to choose an appropriate region of the data for the fitting. When the coincidence efficiency function was measured by using the sources with different self-absorptions, the shape of the function was difficult to recognise because of the scattering of data points within the standard deviation. However, a swelling was clearly recognised at near 0.2 of $(1\text{-}\varepsilon_\beta)/\varepsilon_\beta$ in the result by computer discrimination method. Two fittings over wide region and narrow region of the data brought about 2% difference in disintegration rate. Therefore, we had to consider the reason why the swelling appeared. The reason was estimated from the spectrum measured by the $4\pi\beta$(ppc) shown in Fig. 5-27.

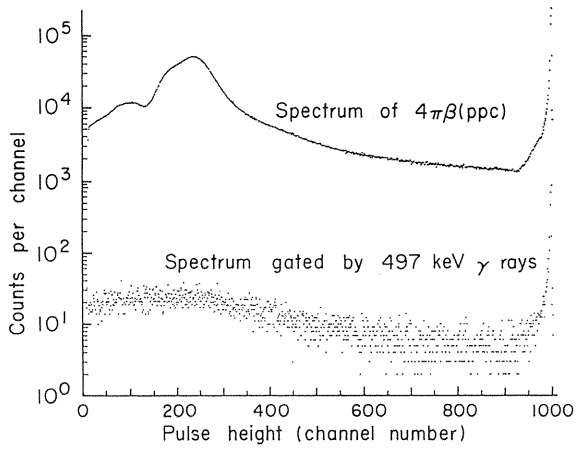

Fig. 5-27. A spectrum of ^{103}Ru obtained from the $4\pi\beta$(ppc) and that gated by the 497 keV γ-rays. The lower energy peak corresponds to the K conversion electrons, and the higher peak to the L conversion electrons and the K conversion plus K Auger electrons.

First of all, considering the coincidence efficiency function, the following equation is obtained by applying Eq. (3-8) to ^{103}Ru.

$$\frac{n_\beta \cdot n_\gamma}{n_c} = n_0 \Big[1 + P_K + P_L + \frac{1-\varepsilon_\beta}{\varepsilon_\beta} \Big[1 - \sum a_k c_k \Big\{ 1 - \Big(\frac{\alpha\varepsilon_{ce} + \varepsilon_{\beta\gamma}}{1+\alpha} \Big)_k \Big\} + P_K(1-C_K) + P_L(1-C_L) \Big] \Big] \tag{5-33}$$

$$C_K = \frac{1-\varepsilon_K}{1-\varepsilon_\beta}, \quad C_L = \frac{1-\varepsilon_L}{1-\varepsilon_\beta}$$

where P_K is the probability that K internal conversion electron with energy of about 17 keV and non-detected K X-ray are emitted, and P_L is the probability that L internal conversion electron with energy of about 37 keV or K internal conversion electron and the successive K Auger-electron are emitted. ε_K and ε_L are the probabilities to detect above each phenomenon and other notations are the same as before. If C_K and C_L are constant or smaller enough than unity, the coincidence efficiency function is linear. At high ε_β region ε_K and ε_L are nearly

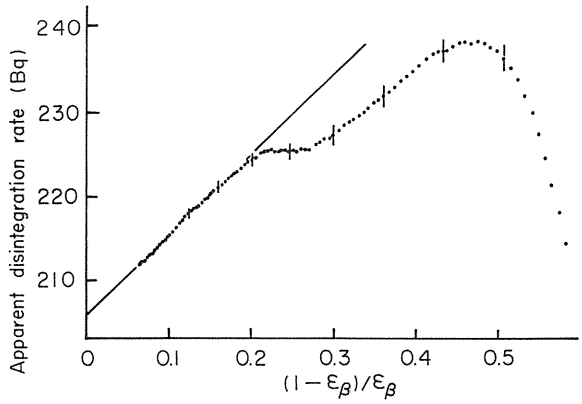

Fig. 5-28. A coincidence efficiency function of a ^{103}Ru source prepared by electrospraying method. The source showed the highest detection efficiency of about 94%.

Table 5-8. Emission probabilities for the 497 keV γ-rays of ^{103}Ru, calculated from the disintegration rates obtained under the assumption of three kinds of decay scheme.

Run	γ-ray detection efficiency ($\times10^{-3}$)	Source	n_γ/n_0 ($\times10^{-3}$) Ref.36	Mean	γ-ray emission probability Ref.36	Ref.35	Ref.34
1	3.4393 (194)	1	3.1628 (150)*				
		2	3.1360 (150)	3.1380	0.9124	0.9170	0.9186
		3	3.1400 (150)	(106)	(58)	(58)	(58)
2	3.4163 (196)	4	3.1126 (150)				
		5	3.1379 (150)	3.1282	0.9157	0.9203	0.9219
		6	3.1280 (150)	(90)	(59)	(59)	(59)
3	3.4327 (196)	7	3.1195 (150)				
		8	3.1147 (150)	3.1191	0.9086	0.9132	0.9147
		9	3.1230 (150)	(90)	(58)	(58)	(58)
4	3.4212 (194)	10	3.1106 (150)				
		11	3.1186 (131)	3.1157	0.9107	0.9153	0.9169
		12	3.1180 (150)	(90)	(57)	(57)	(57)
				Mean	0.9119 (29)	0.9165 (29)	0.9180 (29)

* This data was omitted.

Table 5-9. The final result for the emission probabilities of the 497, 557 and 610 keV γ-rays. The relative intensities agree with the values reported in reference 36.

Run	497 keV	557 keV	610 keV
1	0.9152 (58)	0.008398 (130)	0.05800 (45)
2	0.9185 (59)	0.008460 (123)	0.05838 (53)
3	0.9114 (58)	0.008744 (110)	0.05800 (49)
4	0.9135 (57)	0.008519 (109)	0.05781 (44)
Mean	0.9147 (29)	0.008530 (59)	0.05805 (24)
Relative intensity	1000	9.33	63.5

unity, then C_K and C_L are zero and the slope is constant. When the discrimination level, however, rises above 10 keV as seen in the spectrum shown in Fig. 5-27, ε_K decreases and large C_K introduces small slope. When the discrimination level rises further, $(1\text{-}\varepsilon_K)$ approaches to unity and small change of $(1\text{-}\varepsilon_\beta)$ brings C_K to be constant. When the discrimination level rises above 20 keV, ε_L begins to decrease and the increase of C_L leads to decrease in the slope. These change gives the coincidence efficiency function shown in Fig. 5-26.

In order to obtain reliable extrapolation the shape in the region which has not been measured seems to be important. Although the slope of coincidence efficiency function was considered to be probably constant from the above discussion, the slope was actually examined using the source with small self-absorption prepared by electrospraying method[40]. From the result shown in Fig. 5-28 the disintegration rate can be determined by extrapolation of the fitting function at the region from 0.1 to 0.2 along horizontal axis. This is supported by the smooth change of spectrum shown in Fig. 5-27. In conventional coincidence counting thus undulate efficiency function had not been recognised because of statistical error and the superficial-gentle slope perhaps had given systematically larger disintegration rate than true one similar to the case in wide fitting shown in Fig. 5-26. Therefore, the disintegration rates were determined by narrow fitting.

Table 5-8 shows the emission probability for the 497 keV gamma-rays calculated under the assumptions of three kinds of decay scheme evaluated in the Nuclear Data Sheets[34-36]. No beta transition to the ground state was assumed for the decay scheme evaluated in the Nuclear Data Sheets of 1979[35]. The calculated probability agreed considerably with the value described in the Nuclear Data Sheets of 1985, but there were some inconsistency in it. Namely, beta-ray transition to the ground state was calculated to be 0.0134 from gamma-ray intensities, and this value differed from 0.0087 given in the Nuclear Data Sheets by 0.0047. Then the 497 keV transition probability was determined to be 0.9167 from the 497 keV gamma-ray emission probability of 0.9119 by calculation using the internal conversion coefficient of 0.00526. This procedure gave the value of beta-ray transition probability to the ground state to be 0.0103. The difference between this value and assumed one was 0.0031.

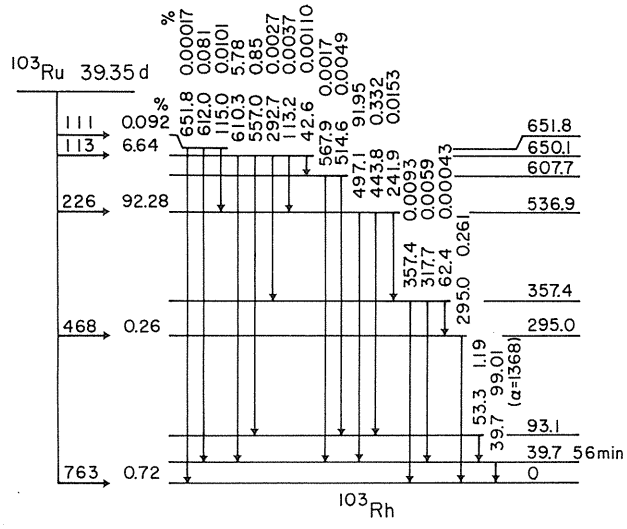

Fig. 5-29. A decay scheme of ^{103}Ru calculated from the present data for the 497 keV γ-rays and the data reported by Macias et al.[39] for the relative γ-ray emission probabilities.

When the calculation was repeated till the result agreed with assumed one, the emission probability for the 497 keV gamma-rays was 0.9147 ± 0.0058 and the beta-ray transition probability to the ground state was calculated to be 0.0072 ± 0.0062. The accompanied large uncertainty was due to the mutual influence in the determinations of disintegration rate and gamma-ray emission probability. On the other hand, when the calculation was repeated under the assumptions that there was no beta transition to the ground state and some to the 40 keV metastable level, the final value of beta transition to the 40 keV level was negative. These results showed that beta-ray transition is not to the 40 keV metastable state but to the ground state.

The emission probabilities for the 497, 557 and 610 keV gamma-rays calculated using this value are shown in Table 5-9. The relative intensities agreed very well with the reported values[36]. Then, Fig. 5-29 is the proposed decay scheme of ^{103}Ru calculated from the present data for the 497 keV gamma-rays and the data reported by Macias et al.[39] for the relative gamma-ray emission probabilities. In the present decay scheme, the important points are that beta transition to the 40 keV metastable state is nothing and that the present value of beta-transition to the ground state is obtained self-consistently.

5. 7. *Measurement of the emission probability for the 1525 keV gamma-rays of* ^{42}K

A feature of this apparatus is the capability of simultaneous measurements of the disintegration rate and the gamma-rays of a source. In customary method of determining emission probability for gamma-rays, the disintegration rate and gamma-ray intensity has been measured by using different apparatuses[1-3], therefore, the nuclides must have relatively long half-lives. With this apparatus, on the other hand, it is possible to determine the emission probability even for the nuclide which has not so long half-life, because the apparatus allows to measure simultaneously both values, the gamma-ray intensity and the disintegration rate. The emission probability for the 1525 keV gamma-rays of ^{42}K ($T_{1/2}$ = 12.3 h) was investigated.

A generator is now available with which ^{42}K can be "milked" from ^{42}Ar ($T_{1/2}$ = 33 y), free from radionuclidic impurities and with a yield of around 140 kBq per day. This activity level is safe and sufficient for many applications which would be brought on account of the effective half-life of 33 y. The generator mode of production of ^{42}K ensures radionuclidic purity, whereas reactor-produced ^{42}K contains almost invariably some ^{24}Na which has a longer half-life (15 h) and emits more intense and higher-energy gamma-rays. The ^{42}K generator was developed at the Technical University of Munich, FRG[41]; the system used in the current experiments was given to Japan Radioisotope Association by Professor Morinaga, and functioned satisfactorily throughout these studies.

A charged-particle accelerator was used to produce ^{42}Ar by means of the ^{40}Ar (^{3}H, P) reaction, and this radionuclide was stored with ^{40}Ar in a stainless steel vessel[41]. The generator contained approximately 180 kBq of activity, which permitted the extraction of about 140 kBq of the daughter activity (^{42}K) per day. This extraction process involved the electrostatic collection of potassium ions onto a stainless steel electrode held at −90 V. The electrode was removed from the generator without affecting the argon, so that the ^{42}K could be dissolved in distilled water with about 100 μl and dispersed onto the metallised VYNS films used for $4\pi\beta$ proportional counting. The bi-dimensional mode was initially adopted to obtain the source activity, followed by the gamma-ray counts. These two types of measurement were repeated 40 times, with a 1000 s counting time for each measurement.

Fig. 5-30 shows a typical activity measurement obtained by changing the discrimination level, in which the apparent disintegration rate is seen to decrease when $(1-\varepsilon_\beta)/\varepsilon_\beta > 0.03$. This is almost certainly due to the contributions from bremsstrahlung, and restricts the range

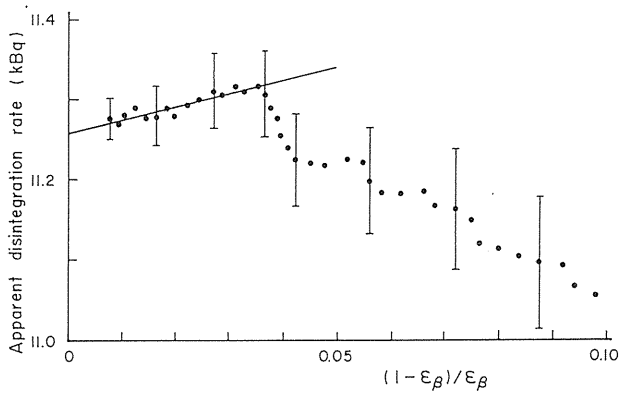

Fig. 5-30. An example of coincidence efficiency function of ^{42}K derived by the computer discrimination method for the gate set of the 1525 keV γ-rays.

Table 5-10. Emission probability for the 1525 keV γ-rays of ^{42}K.

Run number	Disintegration rate (Bq)	Peak area (cps)	Detection efficiency ($\times 10^{-3}$)	Emission probability
1	13068±10	2.7900±0.0128	1.1842±0.0073	0.18029±0.00139
2	16986±12	3.6402±0.0151	1.1880±0.0072	0.18039±0.00134
3	23021±18	4.8240±0.0120	1.1622±0.0071	0.18030±0.00120
4	9574.2±7.9	2.0360±0.0072	1.1674±0.0071	0.18216±0.00128
Mean				0.18079±0.00087

of linear fitting of the data as shown. The ^{42}K gamma-ray data were accumulated over about 4×10^4 s, and bremsstrahlung effects were only noted below 300 keV.

Table 5-10 lists the data used to determine emission probability for the 1525 keV gamma-rays of ^{42}K; the uncertainties in the detection efficiencies were calculated from the statistical uncertainties related with other factors and the systematic uncertainties as estimated for the calculation of the areas of the pulse height peaks. The systematic uncertainties were described in section 4.2. The four sets of measurements produced data with sufficiently good agreement each other and gave a recommendable emission probability of 0.1808 ± 0.0009 calculated as their arithmetic mean.

Table 5-11 lists the result from the present work and the various reference values of the emission probability of the 1525 keV gamma-rays (the most recent reference one is old more than 28 years). The data in the table agree within their specified uncertainties, but only the present result has an uncertainty that is small enough to use ^{42}K as a suitable source for accurate detector calibrations. Although a single most important reason for achieving this improvement was the availability of ^{42}K free from ^{24}Na, the present procedure of employing coincidence counting with live-timed bi-dimensional data acquisition also contributed to bring the greater accuracy.

Table 5-11. The final result for the emission probability of the 1525 keV γ-rays compared with published results. Mackin and Love reported their uncertainties at the 3σ confidence level, and their value has been divided by three.

Author	Emission Probability
Emery et al. (42)	0.178±0.009
Mackin et al. (43)	0.184±0.005
Persson (44)	0.179±0.005
Present work	0.1808±0.0009

A tentative decay scheme can be calculated for ^{42}K on the basis of the emission probability of the 1525 keV gamma-rays and the relative gamma-ray branching ratios quoted by Kawade et al.[45] The resulting decay scheme is shown in Fig. 5-31, where the Q_β value was obtained from the Table of Isotopes[46], and the half-life was the data by Kawade[47]. Both the energy of the 2753 keV nuclear level and the gamma-ray intensities associated with this level were not accurately determined.

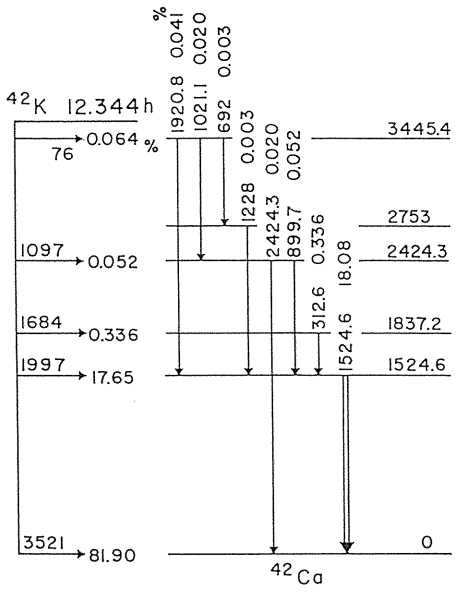

Fig. 5-31. A decay scheme of ^{42}K calculated from the present data for the 1525 keV γ-rays and the data reported by Kawade et al.[45]

6. Conclusion

The operation of a $4\pi\beta$(ppc)-γ(HPGe) coincidence counting apparatus using the live-timed bi-dimensional data acquisition system can bring acceptably accurate measurement of gamma-ray emission probability. In the customary method, the disintegration rates and gamma-ray intensities of standard sources and sample sources were measured at separate places in different times by different plural researchers. However, it is required for achievement of high-accuracy measurement that the same investigators measure them at the same laboratory in the same time and remeasure for questionable sources immediately. This is the very system to satisfy these requirements.

Easy application of computer discrimination method makes it possible to determine the disintegration rate from short-time measurement; furthermore, application of the HPGe detector as a gamma-ray detector makes it possible to obtain the coincidence with gamma-rays having arbitrary many different energies. Therefore, two-dimensional extrapolation method developed by Smith and Stuart is simply applied for ^{57}Co which emits many low-energy conversion electrons. The disintegration rate of ^{152}Eu which is difficult to measure can be determined by developing this method. Also the disintegration rate of ^{133}Ba can be obtained easily and it was proved that the gamma-gate set carried out customarily in the $4\pi\beta$-γ coincidence counting gave smaller disintegration rate by 0.5% with the maximum.

The result of emission probability for ^{59}Fe gamma-rays, obtained to verify the propriety of the measuring method, proved that the gamma-ray emission probability could be determined with uncertainty of about 0.5% from several measurements. The emission probabilities for the 1099 and the 1292 keV gamma-rays of ^{59}Fe were 0.5665 ± 0.0022 and 0.4302 ± 0.0029, respectively. Since the beta branching ratio to the ground state is as small as 0.2%, there was few advantages to use this system. However, usefulness of this system has been supremely exhibited for the nuclides transiting directly to the metastable or the ground state.

About 90% of ^{86}Rb transit to the ground state and the remainder emit the 1077 keV gamma-rays following beta decay. The measured result of the emission probability for the gamma-rays was 0.0887 ± 0.0003 which was more accurate than the reported values.

The 40 keV level of ^{103}Rh followed by beta transition of ^{103}Ru is metastable and the transition from it mostly appeared in a form of internal conversion electron; therefore, it is difficult to determine the disintegration rate. Another problem is that the existence of beta transition to the metastable state or the ground state is not clear. The present result suggested the existence of the beta transition only to the ground state. The emission probabilities for the principal 497, 557 and 610 keV gamma-rays were 0.9147 ± 0.0058, 0.0085 ± 0.0001 and 0.0581 ± 0.0005, respectively.

Lastly, the emission probability for the 1525 keV gamma-rays of ^{42}K which decays with half-life of about 12 h was measured, and it was 0.1808 ± 0.0009. This ^{42}K can be milked from ^{42}Ar with half-life of 33 y and has no impurity, then it will be expected to apply to various fields containing calibration of gamma-ray detector.

This system stores the data on a magnetic tape because of small size of the memory available in the micro-computer, but it is important that faster accumulation and calculation is introduced by direct storage of data in a large-memory computer. If fast ADCs are used, the source with high disintegration rate can be measured at the large distance between source and gamma-ray detector and this fact results in the decreases of cascade-summing effect and of uncertainty due to geometrical reproducibility.

Acknowledgements

The authors would like to thank Associate Professor K. Kawade for his helpful suggestions in application of bi-dimensional data acquisition system and for his advice to the measurement of ^{42}K decay and Dr. G. C. Lowenthal for his encouragement. They also would like to thank Emeritus Professor T. Watanabe, Dr. T. Aoyama and Mr. S. Hirokawa for their comments, Mr. K. Yanagida for his kind help in making the counter and the electronic circuits, and Messrs. S. Kitaori and Y. Nozue for their help with experiments. They are also indebted to the Japan Radioisotope Association for lending the ^{42}Ar-^{42}K generator and Radioisotope Center in Nagoya University for allowing preparation of some sources. This work was partly supported by a Grant-in-Aid for Scientific Research from the Ministry of Education, Science and Culture.

References

1) U. Schotzig, K. Debertin and K. F. Walz, *Int. J. Appl. Radiat. Isotopes* **28** (1977) 503.
2) R. J. Gehrke, R. G. Helmer and R. C. Greenwood, *Nucl. Instr. and Meth.* **147** (1977) 405.
3) Y. Yoshizawa, Y. Iwata, T. Katoh, J. Ruan and Y. Kawada, *ibid.* **212** (1983) 249.
4) H. Miyahara, S. Kitaori and T. Watanabe, *Appl. Radiat. Isotopes* **38** (1987) 793.
5) D. Smith, *Metrologia* **11** (1975) 73.
6) H. Miyahara, M. Watanabe and T. Watanabe, *Nucl. Instr. and Meth.* **A251** (1986) 156.
7) M. Yoshida, H. Miyahara and T. Watababe, *Int. J. Appl. Radiat. Isotopes* **28** (1977) 633.
8) A. Gandy, *ibid.* **11** (1961) 75.
9) P. J. Campion, *ibid.* **4** (1959) 232.
10) A. P. Baerg, *Metrologia* **2** (1966) 23.
11) A. P. Baerg, *ibid.* **3** (1967) 105.
12) M. Dojo, *Nucl. Instr. and Meth.* **115** (1974) 425.
13) R. G. Helmer, *ibid.* **199** (1982) 521.
14) K. Debertin and U. Schotzig, *ibid.* **158** (1979) 471.
15) S. Brandt, *Statistical and Computation Methods in Data Analysis* (North-Holland, Amsterdam, 1976).
16) D. Smith and L. E. H. Stuart, *Metrologia* **11** (1975) 67.
17) K. Debertin, *Nucl. Instr. and Meth.* **158** (1979) 479.
18) Y. Yoshizawa, Y. Iwata and Y. Iinuma, *ibid.* **174** (1980) 133.
19) J. Legrand, C. Clement and C. Bac, *Bull. BNM* **6** (19) (1975) 31.
20) U. Schotzig and K. Debertin, *PTB report* **Ra-10** (1980).
21) S. Baba, S. Ichikawa, T. Sekine, I. Ishikawa and H. Baba, *Nucl. Instr. and Meth.* **203** (1982) 273.
22) B. Schauvenet, J. Morel and J. Legrand, *Int. J. Appl. Radiat. Isotopes* **34** (1983) 479.
23) A. Rytz, *CCEMRI* (II)/**85-1** (1985).
24) Yu. V. Sergeenkov and V. M. Sigalov, *Nuclear Data Sheets* **49** (1986) 639.
25) S. Raman, H. Kawakami, S. Ohya and Z. Matumoto, *Phys. Rev.* **C9** (1974) 2463.
26) H. Miyahara and T. Watanabe, *Appl. Radiat. Isotopes* **36** (1985) 75.
27) J. Legrand, J. Morel and C. Clement, *Nucl. Phys.* **A142** (1970) 63.
28) S. C. Pancholi, J. J. Pinajian, N. R. Johnson, A. Kumar, S. K. Soni, M. M. Bajaj, S. L. Gupta and N. K. Saha, *Phys. Rev.* **C8** (1973) 2277.
29) NCRP, *Report* **No.58** 2nd edition (1985).
30) H. Miyahara, T. Momose and T. Watanabe, *Appl. Radiat. Isotopes* **37** (1986) 1.
31) P. J. Campion, J. G. V. Taylor and J. S. Merritt, *Int. J. Appl. Radiat. Isotopes* **8** (1960) 8.
32) H. W. Jr. Brandhorst and J. W. Cabble, *Phys. Rev.* **125** (1961) 1323.

33) V. G. Gupta, P. K. Srivastava and D. G. Sarantites, *Nucl. Phys.* **73** (1965) 413.
34) D. C. Kocher, *Nuclear Data Sheets* **13** (1974) 337.
35) B. Harmatz, *ibid.* **28** (1979) 403.
36) D. De Frenne, E. Jacobs and M. Verboven, *ibid.* **45** (1985) 363.
37) H. Pettersson, S. Antman and Y. Grunditz, *Z. Phys.* **233** (1970) 260.
38) M. Ohshima, Z. Matumoto and T. Tamura, *J.Phys. Soc. Jpn.* **51** (1982) 43.
39) E. S. Macias, M. E. Phelps, D. G. Sarantites and R. A. Meyer, *Phys. Rev.* **C14** (1976) 639.
40) D. J. Carswell and J. Milsted, *J. Nucl. Energy* **4** (1957) 51.
41) H. Wegmann, E. Huenges, H. Muthig and H. Morinaga, *Nucl. Instr. and Meth.* **179** (1981) 217; H. Muthig, Doctorate thesis, The Technical University of Munich (1984).
42) E. W. Emery and N. Veall, *Proc. Phys. Soc.* **A68** (1955) 346; *ibid.* **72** (1958) 675.
43) J. Mackin and D. Love, *J. Inorg. Nucl. Chem.* **10** (1959) 17.
44) B. Persson, *Acta Radiol.* **58** (1962) 192.
45) K. Kawade, H. Yamamoto, K. Yoshikawa, K. Iizawa, I. Kitamura, S. Amemiya and T. Katoh, *J. Phys. Soc. Jpn.* **29** (1970) 43.
46) C. M. Lederer and V. S. Shirley, *Table of Isotopes* 7th edition (Wiley, New York, 1978).
47) K. Kawade, private communication.